

VISUALIZACION Y COMPARACION
DE RADIOSONDEOS
ATMOSFERICOS TROPICALES

FACULTAD DE
INGENIERIA

Universidad Central de Venezuela



UNIVERSIDAD CENTRAL DE VENEZUELA
FACULTAD DE INGENIERIA
ESCUELA DE INGENIERIA CIVIL
DEPTO DE INGENIERIA HIDROMETEOROLOGICA
LABORATORIO DE HIDROMETEOROLOGIA

VISUALIZACION Y COMPARACION DE RADIOSONDEOS
ATMOSFERICOS TROPICALES

BREVE RESEÑA DEL PROYECTO Y GUIA PARA USO DEL
DISKETTE DEMO-TEMP

Primera versión sujeta a mejoras

Por:

Prof. Luis G. Hidalgo P

Programa elaborado con datos provenientes
del Servicio de Meteorología de la Fuerza Aérea
de Venezuela mediante telecomunicaciones entre
el CRT (Maracay) y Universidad Central (Caracas)
durante los meses de marzo, abril y mayo 1993

Caracas-Ciudad Universitaria, mayo de 1993

BREVE RESEÑA DEL PROYECTO
DE INVESTIGACION

INTRODUCCION: Existe una red de estaciones meteorológicas de aire superior que incluye estaciones en el área tropical de las Américas. La estaciones efectúan mediciones al menos una vez al día. Se obtienen perfiles verticales de presión, temperatura, humedad, dirección y velocidad del viento. El estudio y comparación de estos perfiles permite determinar el estado atmosférico con respecto a varios factores, uno de ellos es la presencia de características que permitan definir el perfil como perteneciente a la temporada de lluvias o a la temporada de sequía. Se supone que el tiempo en áreas tropicales presenta las épocas de sequía, lluvias y transiciones.

OBJETIVOS: El objetivo del proyecto es el desarrollo de un software que permita el almacenamiento de datos de radiosondeos y que, mediante un conjunto de algoritmos, permita clasificar el patrón de temperatura, punto de rocío, energía total y temperaturas potenciales, para luego determinar si un sondeo particular puede definirse como perteneciente a la temporada de sequía o la de lluvias o transición. La aplicación de coeficientes de correlación podría incluirse para el reconocimiento de patrones y comparaciones con situaciones pasadas.

RECURSOS: Para la realización de la investigación se necesitan conjuntos de datos de radiosondeos de la región tropical panamericana (80°W a 60°W), un computador con capacidad de graficado preferiblemente con pantalla VGA. El acceso en tiempo real a la red mundial de telecomunicaciones es necesario.

METODOLOGIA: Escogencia de las variables básicas y derivadas para construir los perfiles verticales. Recolección de datos de radiosondas de estaciones diversas tropicales. Procesamiento de cada radiosonda. Visualización de los perfiles. Selección de radiosondas patrones. Clasificación de radiosondas de acuerdo a los patrones. Elaboración de perfil de estabilidad por capas. Visualización geográfica de los tipos de patrones y las fechas. Agregado de información de nubes y lluvias. Conclusiones sobre la concordancia entre datos de nubes, lluvias, patrones, clases de patrones y situación general.

TIEMPOS: 15 de mayo de 1993 al 15 de mayo de 1994

BIBLIOGRAFIA: Holton, J. Introduction to Dynamic Meteorology.

16/mayo/1993

GUIA PARA EL USO DEL DISKETTE

DEMO - TEMP

El diskette DEMO-TEMP contiene archivos que permiten visualizar y comparar perfiles verticales atmosféricos de presión, temperatura y humedad mediante un programa denominado TEMP007.EXE que es activado por un programa tipo BAT denominado TEMP.BAT. Los datos de radiosondas (o sondeos por radio) están contenidos en archivos separados, una para cada sondeo. El diskette DEMO-TEMP contiene una muestra de 10 sondeos tropicales, los cuales pueden ser observados dibujados en pantalla.

Si se desea imprimir en papel los diagramas termodinámicos que el programa TEMP007.BAS elabora en pantalla, antes de correr TEMP, es necesario correr el programa auto-ejecutable GRAPHICS. Si la tarjeta de video es Hércules es necesario correr, antes del programa TEMP, el programa MSHERC para tener acceso a la capacidad de graficado de la pantalla. Las demás tarjetas de video activan la capacidad de graficado (pixels) en forma automática.

Prueba de diskette DEMO-TEMP

=====

Para efectuar una prueba simple del diskette DEMO-TEMP se siguen las siguientes instrucciones y se usan sólo dos teclas ENTER y ESCAPE.

En las siguientes explicaciones ? significa presionar la tecla ENTER y se usa para adelantar un paso en la corrida del programa o para seleccionar una opción por default. El símbolo ? significa presionar la tecla ESCAPE o Esc y se usa en el paso correspondiente a selección de nombre de archivo.

Paso 1: Coloque el diskette en el drive A

Paso 2: Ejecutar el programa TEMP (hacer A>TEMP ?)

Paso 3: Observar la pantalla donde aparece una identificación relacionada con el software luego ?

Paso 4: Entrada de la letra del drive en uso, la opción default es A y se obtiene con ?.

Paso 5: Entrada del tipo de eje vertical para el diagrama termodinámico. El default eje Z se obtiene con ?.

Paso 6: Selección de trabajo con un radiosonda o con varios. La selección por default es un radiosonda y se obtiene con ?.

Paso 7: Entrada del tipo de video de su computador. La selección por default se obtiene con ? es la número 12 que en VGA es alta resolución casi ortogonal.

Paso 7: Selección del nombre del archivo o radiosondeo. La opción por default es ? (Esc) y asigna el nombre BE2304.931 que es un sondeo efectuado en BELEM el 23 de abril de 1993 a las 1200Z.

Paso 8: Observar la pantalla con los datos del archivo

BE2304.931, luego ?.

Paso 9: Observar en la pantalla la segunda parte de los datos del archivo BE2304.931, luego ?.

Paso 10. Observar en la pantalla primera parte de la Tabla 1 con datos calculados, luego ?.

Paso 11. Observar en la pantalla la segunda parte de la Tabla 1 con datos calculados, luego ?.

Paso 12. Observar en la pantalla la primera parte de la Tabla 2 con datos calculados, luego ?.

Paso 13. Observar en la pantalla el gráfico con los perfiles verticales de temperatura potencial (TPD), temperatura potencial equivalente (TPE), temperatura potencial equivalente máxima (TPEA), temperatura (T), temperatura del punto de rocío (TD), energía total (H) y agua precipitable (WP). Luego ?.

Archivo con instrucciones para usar DEMO-DISKETTE:

Los siguientes tres archivos contienen datos sobre el proyecto de desarrollo de software, la guía del programa y aspectos generales del Laboratorio de Hidrometeorología.

BREVE (Reseña sobre el Laboratorio de Hidrometeorología)
PROYECT (Reseña sobre Visualización y Comparación de Sondeos)
README.WS4 (Instrucciones para usar DEMO-DISKETTE)

Archivos de programas:

TEMP.BAT (para correr el TEMPO07.EXE)
TEMPO07.BAS (listado del programa en ASCII)
TEMPO07.EXE (programa TEMPO06 auto-ejecutable)
CONSTANT.BAS (contiene las constantes termodinámicas del aire)
DEFAULT.BAS (contiene un nombre de archivo de sondeo)
PARGRA.BAS (contiene los parámetros para definir graficado)

Archivos que contiene nombres de sondeos:

BANK.BAS (contiene todos los nombres de sondeos en DEMO-TEMP)
NLOOP.BAS (contiene nombres de sondeos para loop)

Un nombre de sondeo se construye con un esquema SSDDMM.AAN donde:
SS es un indicador de localidad (por ejemplo SL es Salvador (Brasil), DD es el día, MM es el mes y AA es el año y N es la hora del sondeo (08:00 UTC es 1, 11:00 UTC es 2, 14:00 UTC es 3, 17:00 UTC es 4, 20:00 UTC es 5, 23:00 es 6, 02:00 UTC es 7, 05:00 UTC es 8 y el 9 se usa para otra hora no sinóptica).

Archivos con datos de sondeos
=====

Son varios y pueden ser colocados tantos archivos como se quiera, dependiendo de la capacidad del diskette y del computador. Ejemplos:

PV1705.931, SV2504.931, BE2304.931, BS2704.931, SO2704.931
BS0505.931, SV1405.931, BS1604.931, PA2705.931, SV2405.931

La estructura de estos archivos es similar. Esta estructura puede ser observada usando cualquier procesador de palabras en la modalidad no documento (ASCII) con cualquier archivo, por ejemplo el BS0505.931 (Base Sucre 5 de mayo de 1995 1200Z).

Cada archivo de sondeo contiene datos de un radiosondeo específico en ASCII. Los archivos de sondeos pueden ser creados, eliminados, copiados, reformados mediante el uso de cualquier procesador de palabras. Nosotros usamos WS. Cuando se desea colocar un radiosondeo nuevo, se toma un radiosondeo cualquiera, por ejemplo, BS2704.931, se copia con un nombre nuevo y se modifica su contenido colocando nuevos datos.

Directorio de nombres de sondeos disponibles BANK.BAS:
=====

Los nombres de los archivos de radiosondeos se colocan en el archivo BANK.BAS para que puedan ser accedidos por el programa TEMPO07.EXE. Si se adiciona al diskette un nuevo archivo de radiosondeo y no se coloca en BANK.BAS no podrá ser procesado por TEMPO07.EXE. La estructura del archivo BANK.BAS puede ser observada usando cualquier procesador de palabra en la modalidad no documento (ASCII).

Archivo de nombres para LOOP de gráficos NLOOP.BAS
=====

Los nombres de los archivos de radiosondeos que se desean ver en la pantalla en forma de LOOP se colocan en el archivo NLOOP.BAS. La forma de colocar en los datos del archivo NLOOP.BAS está indicada dentro del archivo y puede ser observada usando cualquier procesador de palabras en la modalidad no documento (ASCII).

Archivos con datos de estaciones:
=====

LISTADOS (Indicaciones para comprender los listados)
LISTADO1 (Datos de estaciones de Venezuela)
LISTADO2 (Datos de Aeropuertos/Pistas de Venezuela)
LISTADO3 (Datos de estaciones tropicales RW, W y P)
LISTADO4 (Datos de centros de difusión de mensajes)
LISTADO5 (Abreviaturas SS usadas para nombres de archivos)

Estos listados pueden ser modificados usando procesadores de palabras en la modalidad no documento (ASCII),

Archivos para manejo de hardware:

GRAPHICS.COM (Para imprimir gráficos empleando PRINT SCREEN)
GRAPHICS.PRO (Archivo auxiliar de GRAPHICS.COM)
MSHERC.COM (Para usar pantalla MSHERC)

Estos archivos no pueden ser modificados por el usuario ni por el programador de aplicaciones.

Corrida del programa TEMP007.EXE

Para correr el programa TEMP007.EXE se coloca el nombre TEMP a la derecha del prompt A> y se presiona RETURN. Luego se contestan las preguntas que van apareciendo en pantalla. Si se usan las opciones por default se logran observar tablas con datos calculados y ploteo de gráficos relacionados con uno o mas radiosondas. La corrida mas sencilla del programa se puede realizar empleando las teclas ENTER y ESC para selección de las opciones default.

Si en el Paso 7 se escoge el trabajo con varios radiosondas, TEMP006 trabajará con los archivos indicados en el archivo NLOOP.BAS y sólo aparecerán los gráficos de cada sondeo y no las tablas.

Mejoras futuras:

Eliminar la necesidad de colocar los datos de la estación de sondeo dentro del archivo de datos. Colocar colores a diferentes curvas y diferentes áreas con PAINT. Agregar opción de elaboración de gráficos de curvas por separado para observar detalles. Incluir sondeos patrones de aire ecuatorial (marino, terrestre, sequía y lluvia) y tropical (marino, terrestre, sequía, lluvia). Incluir coeficiente de correlación, mensaje SINOP y clasificación de estabilidad Pasquill vs observada, incluir ploteo del viento.

VARIABLES DE ENTRADA:

=====

Los datos de cada sondeo necesarios para que TEMP007.EXE logre procesar un radiosondeo son:

Nombre de la estación

Fecha del radiosondeo

Altitud de la estación Z0 en m

NN: número de niveles del radiosondeo (máximo 99)

P(mb): presión en milibares de cada nivel

T(°C): temperatura del aire de cada nivel

TD(°C): temperatura del punto de rocío de cada nivel

Actualmente no usa viento

VARIABLES DE SALIDA:

=====

Las tablas 1 y 2 están formadas por las siguientes variables:

Z (m): altura de nivel

P(mb): presión del nivel

T(°C): temperatura del aire

TD(°C): temperatura del punto de rocío

TV(°C): temperatura virtual

E(mb): tensión de vapor actual

Q(g/kg): humedad específica

R(g/kg): relación de mezcla

W(mm): agua precipitable acumulada

U(%): Humedad relativa

TPD(°C): temperatura potencial seca

TPM(°C): temperatura potencia de la mezcla

TPE(°C): temperatura potencial equivalente

TPEA(°C): temperatura potencial máxima.

CPT(cal/gramo): calor sensible

LQ(cal/gramo): calor latente

GZ(ca/gramo): energía potencial

HTOTAL(cal/gramo): energía total

Ejemplo de datos de entrada:

=====

A: BE2304.931

SBBE 82193 BELEM 0123S 4829W 16 .

23/ABR/93 1200Z

22

1	1012	25.6	21.9
2	1000	25.2	20.3
3	938	23.6	17.6
4	928	22.6	16.6
5	850	17.8	14.3
6	785	14.4	7.4
7	715	9.4	8
8	700	8.4	5.3
9	674	7.2	1.2
10	635	4.4	2.7
11	572	0	-4.7
12	547	-3.1	-4.4
13	525	-2.9	-8.9
14	500	-4.3	-15.3
15	490	-5.1	-11.1
16	463	-7.5	-22.5
17	400	-15.7	-18.2
18	300	-30.7	-34.4
19	255	-39.9	-45.9
20	200	-51.7	-99.9
21	150	-64.7	-99.9
22	100	-81.5	-99.9

PRESS ENTER TO CONTINUE

SBBE 82193 BELEM 0123S 4829W 16 23/ABR/93 1200Z

K	Z	m	P	hpa	T	°K	TPD	°K	TPM	°K	TPE	°K	TPEA	°K	CPT	cal/gr	LQ	cal/gr	GZ	cal/gr	HTOTAL	cal/gr
1	16	1012	298.8	297.7	297.8	341.8	354.1	1255	170	0	1425	1425										
2	121	1000	298.4	298.4	298.4	338.6	354.2	1253	156	5	1414	1414										
3	684	938	296.8	302.2	302.1	338.8	357.2	1247	141	31	1419	1419										
4	778	928	295.8	302.1	302.0	336.8	354.3	1242	133	36	1412	1412										
5	1538	850	290.9	304.8	304.5	338.2	347.3	1222	125	72	1419	1419										
6	2216	785	287.5	308.1	307.8	331.0	345.6	1208	86	103	1397	1397										
7	3000	715	282.5	311.0	310.5	338.0	340.9	1187	98	140	1425	1425										
8	3176	700	281.5	311.7	311.3	334.6	340.4	1183	83	149	1415	1415										
9	3489	674	280.4	313.8	313.4	331.6	341.4	1178	65	163	1406	1406										
10	3978	635	277.5	316.0	315.4	337.5	340.4	1166	76	186	1429	1429										
11	4824	572	273.1	320.4	320.0	334.5	340.6	1147	49	226	1423	1423										
12	5180	547	270.0	320.8	320.3	336.1	337.8	1134	53	243	1430	1430										
13	5506	525	270.3	324.9	324.5	336.2	343.0	1135	39	258	1432	1432										
14	5892	500	268.9	327.7	327.4	334.9	345.1	1129	24	276	1430	1430										
15	6051	490	268.0	328.6	328.2	339.0	345.4	1126	35	284	1445	1445										

PRESS ENTER TO CONTINUE

SBBE 82193 BELEM 0123S 4829W 16 23/ABR/93 1200Z

K	Z	m	P	hpa	T	°K	TPD	°K	TPM	°K	TPE	°K	TPEA	°K	CPT	cal/gr	LQ	cal/gr	GZ	cal/gr	HTOTAL	cal/gr
16	6495	463	265.6	331.0	330.8	335.2	345.9	1116	14	305	1435	1435										
17	7616	400	257.4	334.5	334.1	341.9	343.7	1082	24	358	1463	1463										
18	9724	300	242.4	342.0	341.9	344.4	345.4	1019	7	457	1482	1482										
19	10857	255	233.3	344.6	344.5	345.5	346.3	980	3	510	1492	1492										
20	12475	200	221.4	350.7	350.7	350.7	351.3	930	0	586	1516	1516										
21	14286	150	208.4	358.4	358.4	358.4	358.5	876	0	671	1547	1547										
22	16662	100	191.6	369.9	369.9	369.9	370.0	805	0	783	1588	1588										

Ejemplo de Tabla 2:

PRESS ENTER TO CONTINUE

SBBE 82193 BELEM 0123S 4829W 16 23/ABR/93 1200Z

K	Z	P	T	TD	TV	E	Q	R	W	U
	m	hpa	°C	°C	°C	hpa	g/kg	g/kg	mm	%
1	16	1012	25.6	21.9	28.6	26.26	16.29	16.56	51.7	80.1
2	121	1000	25.2	20.3	27.9	23.80	14.94	15.16	49.7	74.3
3	684	938	23.6	17.6	26.0	20.11	13.44	13.63	40.8	69.1
4	778	928	22.6	16.6	24.9	18.88	12.75	12.91	39.4	68.9
5	1538	850	17.8	14.3	19.9	16.29	12.00	12.15	29.6	80.0
6	2216	785	14.4	7.4	15.8	10.30	8.20	8.26	22.9	62.8
7	3000	715	9.4	8.0	11.0	10.73	9.38	9.47	16.6	91.0
8	3176	700	8.4	5.3	9.8	8.91	7.95	8.01	15.3	80.8
9	3489	674	7.2	1.2	8.3	6.67	6.17	6.21	13.4	65.6
10	3978	635	4.4	2.7	5.6	7.42	7.30	7.35	10.7	88.7
11	4824	572	0.0	-4.7	0.8	4.32	4.70	4.73	6.9	70.6
12	5180	547	-3.1	-4.4	-2.3	4.41	5.03	5.06	5.7	90.7
13	5506	525	-2.9	-8.9	-2.3	3.12	3.71	3.72	4.7	63.3
14	5892	500	-4.3	-15.3	-3.9	1.87	2.33	2.33	3.9	42.0
15	6051	490	-5.1	-11.1	-4.6	2.63	3.34	3.35	3.6	62.7

PRESS ENTER TO CONTINUE

SBBE 82193 BELEM 0123S 4829W 16 23/ABR/93 1200Z

K	Z	P	T	TD	TV	E	Q	R	W	U
	m	hpa	°C	°C	°C	hpa	g/kg	g/kg	mm	%
16	6495	463	-7.5	-22.5	-7.3	1.01	1.36	1.36	3.0	29.0
17	7616	400	-15.7	-18.2	-15.3	1.46	2.28	2.28	1.8	81.1
18	9724	300	-30.7	-34.4	-30.6	0.33	0.69	0.69	0.3	69.9
19	10857	255	-39.9	-45.9	-39.9	0.10	0.25	0.25	0.1	52.7
20	12475	200	-51.7	-99.9	-51.7	0.00	0.00	0.00	0.0	0.0
21	14286	150	-64.7	-99.9	-64.7	0.00	0.00	0.00	0.0	0.2
22	16662	100	-81.5	-99.9	-81.5	0.00	0.00	0.00	-0.0	2.6

TOTAL PRECIPITABLE WATER = 51.7 mm
VERTICAL NEAR SOIL SURFACE TEMPERATURE VARIATION = -0.4 °C/100m

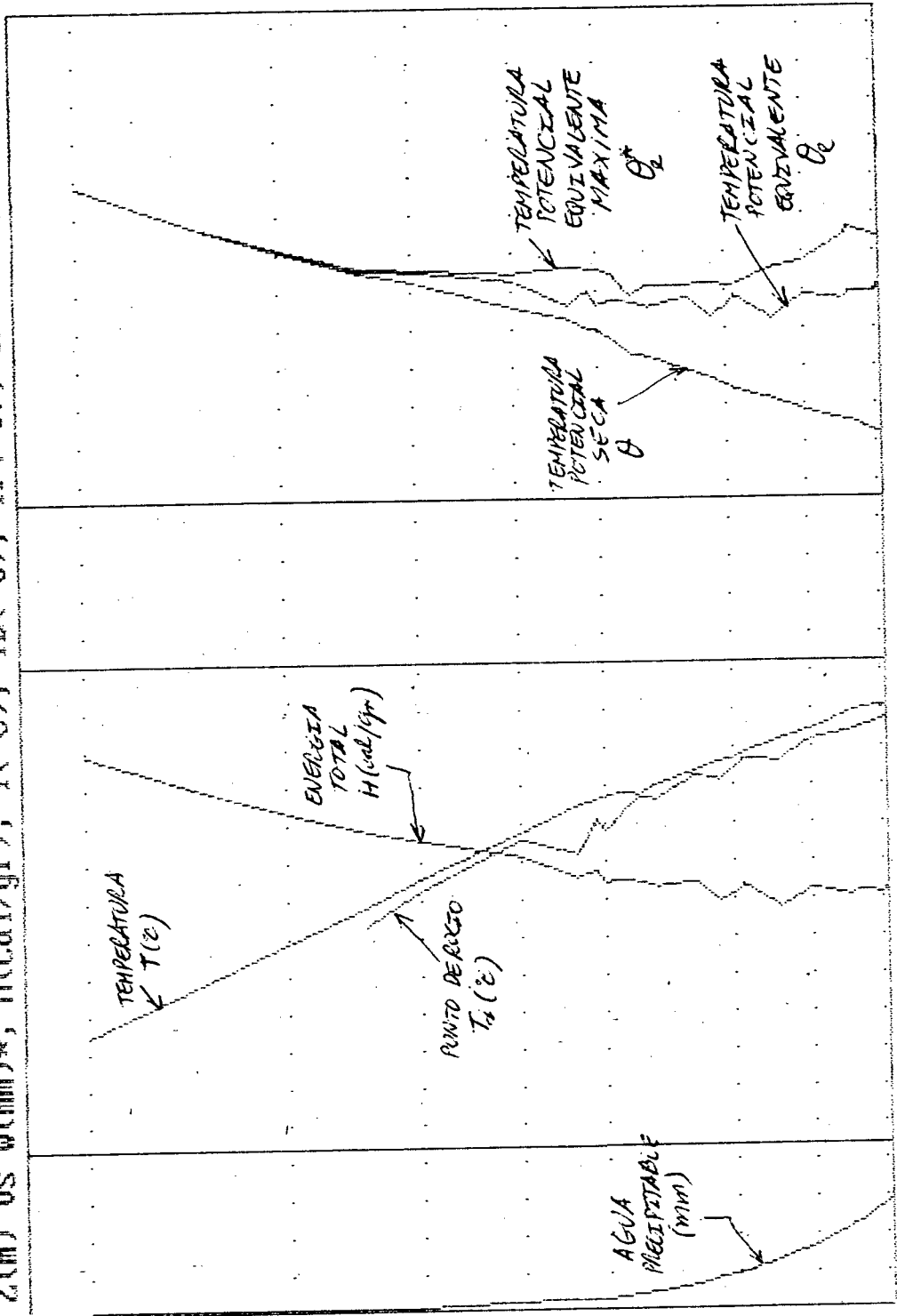
PRESS ENTER TO CONTINUE

A:BE2304.931

SBBE 82193 BELEM 0123S 4829W 16

23/ABR/93 1200Z

Z(m) vs W(mm)*, H(cal/gr), T(°C), TD(°C), TP(°C), TPE(°C), TPE*(°C)



LISTADO DEL PROGRAMA TEMPO07.BAS

```
DECLARE SUB DATADRIVE (DRIVEDATA#)
DECLARE SUB LECTOR (NN, P(), T(), TD())
```

```
1 CLS
REM PROGRAM TEMP FOR VIEWING AND COMPARING RADDS DATA
REM =====
REM PROGRAMMER IS LUIS G HIDALGO
REM NN IS THE NUMBER OF LEVELS IN A RADIOSONDE
REM T ES LA TEMPERATURA EN GRADOS CENTIGRADOS
REM TD ES PUNTO DE ROCIO EN GRADOS CENTIGRADOS
REM P ES LA PRESION ATMOSFERICA EN MILIBARES
REM B ES LA HUMEDAD ESPECIFICA EN GR DE VAPOR POR KG DE AIRE HUMEDO
REM WP ES EL ESPESOR DE AGUA PRECIPITABLE EN MM POR LA FORMULA LINEAR
REM RD ES CONSTANTE DE GAS AIRE SECO EN J/KG/XK
REM GN ES ACELERACION DE LA GRAVEDAD EN M/S2
REM A1,A2,A3,A4,A5,A6,A7 SON CONSTANTES PARA CALCULAR TENSION DE VAPOR
```

```
DIM T(99), TD(99), TV(99), E(99), WW(99), P(99), B(99), Z(99), TPD(99)
DIM ES(99), U(99), R(99), W(99), OPT(99), LB(99), HTOTAL(99)
DIM TPN(99), TPE(99), TPEA(99), RS(99), SZ(99), LOOP$(365)
DIM PF(11)
```

```
REM PROGRAMA PRINCIPAL
REM =====
```

```
2 CLS
GOSUB 500'IMPRESION DE IDENTIFICACION
GOSUB 300
GOSUB 1000'LECTURA LETRA DE DRIVE, CONSTANTES Y PARAMETROS DE GRAFICOS
GOSUB 500'SELECCION DEL TIPO DE EJE VERTICAL
CLS : PRINT "YOU MAY WORK WITH ONE RADIOSONDE OR SEVERAL RADIOSONDES"
INPUT "ONE=ENTER SEVERAL=1": XWORK
CLS : GOSUB 400'NUMERO DE VIDEO
SCREEN PANTALLA
```

```
REM TRABAJO CON UN SOLO ARCHIVO
```

```
REM =====
IF XWORK = 0 THEN
  GOSUB 2000
  RAD# = DRIVE# + "." + FILE#
  OPEN RAD# FOR INPUT AS #1
  GOSUB 10000
  CLOSE #1
END IF
```

```
REM TRABAJO CON VARIOS ARCHIVOS
```

```
REM =====
IF XWORK = 1 THEN
  CALL DATADRIVE(DRIVEDATA#)
  OPEN DRIVEDATA# + "." + "NLOOP.BAS" FOR INPUT AS #1
  INPUT #1, CN#, NLOOP, CM#
  FOR JLOOP = 1 TO NLOOP
    INPUT #1, LOOP$(JLOOP)
    RAD# = DRIVEDATA# + "." + LOOP$(JLOOP)
    OPEN RAD# FOR INPUT AS #JLOOP + 1
    GOSUB 10000
```

```

CLOSE #3: LOOP + 1
NEXT JLOOP
CLOSE #1
END IF
GOSUB 300
INPUT "FOR ANOTHER JOB PRESS THE NUMBER 1 OTHERWISE PRESS ENTER"; X
IF X = 1 THEN GOTO 2
CLS : PRINT "END OF JOB": PRINT DATE#: PRINT TIME#
END

```

```

500 REM SUBROUTINA PARA ESCOGER EL TIPO DE EJE
510 REM =====
CLS
PRINT "KIND OF VERTICAL AXIS SELECTION (DEFAULT IS HEIGHT Z IN METERS)"
INPUT "HEIGHT=1 PRESSURE=2 -LOG(PRESSURE)=3 "; EJE
IF EJE = 0 THEN EJE = 1
IF EJE = 3 THEN
PRINT "-LOG(PRESSURE) IS NOT IMPLEMENTED"
GOSUB 300
GOSUB 500
END IF
RETURN

```

```

600 REM SUBROUTINA DE IDENTIFICACION
610 REM =====
CLS
PRINT "PROGRAM TEMP FOR DISPLAY RADIOSONDE DATA"
PRINT "===== "; PRINT
PRINT "UNIVERSIDAD CENTRAL DE VENEZUELA"
PRINT "FACULTAD DE INGENIERIA"
PRINT "ESCUELA DE INGENIERIA CIVIL"
PRINT "DEPTO. INGENIERIA HIDROMETEOROLOGICA (*)"
PRINT "CIUDAD UNIVERSITARIA - CARACAS 1051"
PRINT "VENEZUELA"; PRINT
PRINT "MOST OF RADIOSONDE DATA COMES FROM THE VENEZUELAN AIR FORCE"
PRINT "WEATHER SERVICE BY TELEPROCESSING BETWEEN SVBS CR-MARACAY"
PRINT "AND THE UNIVERSITY OF CENTRAL VENEZUELA-CARACAS"; PRINT
PRINT "DURING THE JOB, FOR DEFAULT SELECTION JUST PRESS ENTER"; PRINT
PRINT "(*) IS THE REGIONAL WMO CENTER M FOR METEOROLOGICAL TRAINING"
PRINT : PRINT "@ AUTHOR: PROFESOR LUIS G. HIDALGO"
PRINT : PRINT USING "BEGIN OF JOB & &"; DATE#: TIME#
GOSUB 300
RETURN

```

```

STOP
100 REM CALCULO DE TENSION DE VAPOR
110 REM =====
E1 = AA1 * (1 - T1 / T) - AA2 * LOG(T / T1) / LOG(10)
E2 = AA3 * .0001 * (1 - 10 ^ (AA4 * (T / T1 - 1)))
E3 = AA5 * .001 * (10 ^ (AA6 * (1 - T1 / T) - 1))
E4 = AA7: E5 = E1 + E2 + E3 + E4
E5 = 10 ^ (E5)
RETURN

```

```

STOP

```

```

200 REM ORDENAMIENTO DE SERIE
210 REM =====
FOR ORDEN = 1 TO 100
MARCA = 0
FOR K = 2 TO NK
IF P(K) > P(K - 1) THEN
PK = P(K): TK = T(K): TD(K) = TD(K)
P(K) = P(K - 1): T(K) = T(K - 1): TD(K) = TD(K - 1)
P(K - 1) = PK: T(K - 1) = TK: TD(K - 1) = TD(K)
MARCA = 1
END IF
NEXT K
IF MARCA = 0 THEN RETURN
NEXT ORDEN
RETURN

```

```

STOP
300 REM
301 LOCATE 1, 57: PRINT "PRESS ENTER TO CONTINUE"
A$ = INKEY$
LOCATE 2, 57: PRINT "-----"
LOCATE 2, 57: PRINT "*****"
IF A$ = "" THEN GOTO 301
CLS
RETURN

```

```

STOP
400 REM NUMERO DE PANTALLA
410 REM =====
CLS : INPUT "NOW ENTER THE VIDEO SCREEN NUMBER (HERC=3 DEFAULT IS VGA=12)"; PANTALLA
IF PANTALLA = 0 THEN PANTALLA = 12: CLS
RETURN

```

```

STOP
1000 REM LECTURA DE CONSTANTES EN EL ARCHIVO CONSTANT.BAS Y PARGRA.BAS
1010 REM =====
CLS : INPUT "NOW ENTER THE LETTER OF THE DRIVE YOU ARE USING (DEFAULT IS LETTER A)"; DRIVE$
IF DRIVE$ = "" THEN DRIVE$ = "A": CLS
OPEN DRIVE$ + ".:" + "CONSTANT.BAS" FOR INPUT AS #1
INPUT #1, CM$, ND, CM$, PD, CM$, T1, CM$, RD, CM$, GN, CM$, '60
INPUT #1, CM$, AA1, AA2, AA3, AA4, AA5, AA6, AA7
INPUT #1, CM$, MQ2, CM$, MHZ, CM$, LQ40, LQ0, LQ50
INPUT #1, CM$, RW, CM$, CP, CM$, CPV
MV = 2 * MHZ + MQ2: EPSI = MV / ND
CLOSE #1
OPEN DRIVE$ + ".:" + "PARGRA.BAS" FOR INPUT AS #1
INPUT #1, CM$, LARGOX, CM$, LARGOY, CM$, PESO, CM$, MARGEN
INPUT #1, CM$, TMAX, CM$, TMIN, CM$, ZMAX, CM$, ZMIN
INPUT #1, CM$, HTMAX, CM$, HTMIN, CM$, PMAX, CM$, TPMAX
INPUT #1, CM$, TPKIN, CM$, WPMAX, CM$, NNN
INPUT #1, CM$
FOR NPP = 1 TO NNN: INPUT #1, PP(INPP): NEXT NPP
CLOSE #1
RETURN

```

```

STOP
2000 REM LECTURA DE DATOS DE UN RADIOSONDED
2010 REM =====
IF XWORK = 0 THEN INPUT #1, NOMBRE$, FECHA$, Z0, NN
IF XWORK = 1 THEN INPUT #JLOOP + 1, NOMBRE$, FECHA$, Z0, NN
FOR LECTK = 1 TO NN
IF XWORK = 0 THEN INPUT #1, P(LECTK), T(LECTK), TD(LECTK)
IF XWORK = 1 THEN INPUT #JLOOP + 1, P(LECTK), T(LECTK), TD(LECTK)
IF TD(LECTK) = 9999 THEN TD(LECTK) = -99.9
NEXT LECTK
IF XWORK = 0 THEN
CLS
PRINT RAD$
PRINT NOMBRE$
PRINT FECHA$
PRINT NN
FOR JN = 1 TO NN
PRINT JN, P(JN), T(JN), TD(JN)
IF JN = 15 OR JN = 30 OR JN = 45 OR JN = 60 OR JN = 75 THEN GOSUB 300
NEXT JN
END IF
GOSUB 300
GOSUB 200
RETURN

```

```

STOP
3000 REM CALCULOS NIVEL A NIVEL
3010 REM =====
FOR K = 1 TO NN
AA = T1 + TD(K); BB = T2 + T(K)
T = AA; GOSUB 100; E(K) = ES
T = BB; GOSUB 100; ES(K) = ES
B(K) = 1000 * EPS1 * E(K) / (P(K) - .378 * E(K))
R(K) = 1000 * EPS1 * E(K) / (P(K) - E(K))
RS(K) = 1000 * EPS1 * ES(K) / (P(K) - ES(K))
U(K) = 100 * E(K) / (ES(K) + .0001)
DPT(K) = (4.18 / 1000) * CP * (T(K) + T1)
LQ(K) = (4.18 / 1000) * LQ0 * B(K) / 1000
TV(K) = (T(K) + T1) * (1 + R(K) / 1000 / EPS1) / (1 + R(K) / 1000)
TPD(K) = (T(K) + T1) * (1000 / P(K)) ^ (RD / CP)
EXP1 = (RD + R(K) * .001) / (CP + R(K) * .001 * CPV)
TPN(K) = (T(K) + T1) * (1000 / P(K)) ^ EXP1
EXP2 = EXP(LQ0 * R(K) * .001 / (CP * (T(K) + T1)))
TPE(K) = TPD(K) * EXP2
EXP3 = EXP(LQ0 * RS(K) * .001 / (CP * (T(K) + T1)))
TPEA(K) = TPD(K) * EXP3
NEXT K
RETURN

```

```

4000 REM CÁLCULO DE ESPESORES
4010 REM =====
WW = 0; Z(1) = Z0
SZ(1) = 0
FOR K = 1 TO NN - 1
WW(K) = 10 * (P(K) - P(K + 1)) * (B(K) + B(K + 1)) / (2 * BN)

```

```

TVM = (TV(K) + TV(K + 1)) / 2
DELTAZ = RD * TVM * LOG(P(K) / P(K + 1)) / G0
Z(K + 1) = Z(K) + DELTAZ
GZ(K + 1) = (Z(K + 1) - Z0) * G0 * (4.8 / 1000)
WW = WW + WW(K)
NEXT K
RETURN

```

```

4050 REM CALCULO DE ENERGIA TOTAL
4060 REM =====
FOR K = 1 TO NN
HTOTAL(K) = LG(K) + DPT(K) + GZ(K)
NEXT K
RETURN

```

```

5000 REM PERFIL DE AGUA PRECIPITABLE
5010 REM =====
W(1) = WW
FOR K = 2 TO NN
W(K) = W(K - 1) - WW(K - 1)
NEXT K
RETURN

```

```

6000 REM IMPRESION DE DATOS DE SALIDA TABLA 1
6010 REM =====
LDN = LN
JJ = NN / LDN - INT(NN / LDN)
IF JJ > 0 THEN JJ = INT(NN / LDN) + 1
IF JJ = 0 THEN JJ = NN / LDN
FOR J = 1 TO JJ: CLS : PRINT : PRINT
PRINT USING "& &"; NOMBRE$; FECHA$
N1 = (J - 1) * LDN + 1
N2 = (J - 1) * LDN + LDN
IF N2 > NN THEN N2 = NN
PRINT "===== "
PRINT " K   Z       P       T       TD      TV       E       G       R       W       U "
PRINT "      m   hpa   xC     xC     xC     hpa   g/kg   g/kg   mm    % "
PRINT "===== "
FOR K = N1 TO N2: TV(K) = TV(K) - T1
PRINT USING "## ##### ##.# ##.#"; K; Z(K); P(K); T(K); TD(K);
PRINT USING "##.# ##.# ##.# ##.# ##.# ##.# ##.#"; TV(K); E(K); G(K); R(K); W(K); U(K)
IF K = LDN THEN
GOSUB 300
END IF
NEXT K
PRINT "===== "
NEXT J
PRINT USING "TOTAL PRECIPITABLE WATER = ##.# mm"; WW
TVVT = 100 * (T(2) - T(1)) / (Z(2) - Z(1))
PRINT USING "VERTICAL NEAR SOIL SURFACE TEMPERATURE VARIATION = ##.#x°C/100m"; TVVT
IF TVVT < 0 THEN PRINT "SURFACE TEMPERATURE INVERSION"
GOSUB 300
RETURN

```

```

7000 REM IMPRESION DE DATOS DE SALIDA TABLA 2

```

```

7010 REM =====
LDN = 15: JJ = NN / LDN - INT(NN / LDN)
IF JJ > 0 THEN JJ = INT(NN / LDN) + 1
IF JJ = 0 THEN JJ = NN / LDN
FOR J = 1 TO JJ: CLS : LOCATE 3, 1
PRINT USING "& A"; NOMBRE$; FECHA$
N1 = (J - 1) * LDN + 1; N2 = (J - 1) * LDN + LDN
IF N2 > NN THEN N2 = NN
PRINT "-----"
PRINT " K   Z     P     T     TPD  TPM   TPE   TPEA  CPT   LB    GZ   HTOTAL"
PRINT "      #     hpa  xK     xK    xK    xK   cal/gr cal/gr cal/gr cal/gr"
PRINT "-----"
FOR K = N1 TO N2
PRINT USING "## ##### ### ##.#"; K; Z(K); P(K); T(K) + T1;
PRINT USING " ##.# ##.# ##.# ##.# ##.#"; TPD(K); TPM(K); TPE(K); TPEA(K);
PRINT USING "##### ##### ##### #####"; CPT(K); LB(K); GZ(K); HTOTAL(K)
IF K = LDN THEN
GOSUB 300
GOSUB 200
END IF
NEXT K
PRINT "-----"
NEXT J
RETURN

```

```

STOP
7500 REM PLOTED DE NOMBRE DE ESTACION Y FECHA
7510 REM =====
LOCATE 2, 1: PRINT NOMBRE$
LOCATE 3, 1: PRINT FECHA$
RETURN

```

```

STOP
8000 REM PLOTED DE FORMATO DE GRAFICADO
8010 REM =====
IF EJE = 2 THEN LOCATE 5, 12: PRINT "P(mm) vs W(mm)#, H(cal/gr), T(xC), TD(xC), TP(xC), TPE(xC), TPE#(xC)"
IF EJE = 1 THEN LOCATE 5, 12: PRINT "Z(mm) vs W(mm)#, H(cal/gr), T(xC), TD(xC), TP(xC), TPE(xC), TPE#(xC)"
XX0 = MARGEN: XXX1 = MARGEN + LARGOX
YY0 = MARGEN: YY1 = MARGEN + LARGOY
LINE (XX0, YY0)-(XXX1, YY1), B
DELTAP = LARGOX / 12 + 2 * PESO
DELTAG = PESO * DELTAP
XX1 = MARGEN + DELTAP: LINE (XX1, YY0)-(XX1, YY1)
XX2 = XX1 + DELTAP: LINE (XX2, YY0)-(XX2, YY1)
XX3 = XX2 + DELTAP: LINE (XX3, YY0)-(XX3, YY1)
XX4 = XX3 + DELTAG
PIPE = (XX4 - XX3) / (TPMAX - TPMIN)
TAA = (XX2 - XX1) / (TMAX - TMIN)
HHT = (XX2 - XX1) / (HTMAX - HTHIN)
HHTT = XX1 + (XX2 - XX1) / 3
PWF = (XX1 - XX0) / WPMAX
RETURN

```

```

STOP
9000 REM PLOTED DE CURVAS

```

```

9010 REM =====
PAINT (100, 100), 0, 15
FOR K = 1 TO NN - 1
IF EJE = 2 THEN
  Y1 = MARGEN + LARGOY * (P(K)) / (PMAX - PMIN)
  Y2 = MARGEN + LARGOY * (P(K + 1)) / (PMAX - PMIN)
END IF
IF EJE = 1 THEN
  Y1 = MARGEN + LARGOY * (ZMAX - Z(K)) / (ZMAX - ZMIN)
  Y2 = MARGEN + LARGOY * (ZMAX - Z(K + 1)) / (ZMAX - ZMIN)
END IF
TX1 = XX1 + (T(K) - TMIN) * TAA
TX2 = XX1 + (TD(K) - TMIN) * TAA
TX3 = XX1 + (T(K + 1) - TMIN) * TAA
TX4 = XX1 + (TD(K + 1) - TMIN) * TAA
REM PLOTED DE TEMPERATURA
LINE (TX1, Y1)-(TX3, Y2)
REM PLOTED DE PUNTO DE ROCIO
IF TD(K) (<) -99.9 AND TD(K + 1) (<) -99.9 THEN
LINE (TX2, Y1)-(TX4, Y2)
END IF
REM PLOTED DE TEMPERATURA POTENCIAL EQUIVALENTE
M1 = XX3 + (TPE(K) - TPEMIN) * PTPE
M2 = XX3 + (TPE(K + 1) - TPEMIN) * PTPE
LINE (M1, Y1)-(M2, Y2)
REM PLOTED DE TEMPERATURA POTENCIAL EQUIVALENTE MAXIMA
M3 = XX3 + (TPD(K) - TPEMIN) * PTPE
M4 = XX3 + (TPD(K + 1) - TPEMIN) * PTPE
LINE (M3, Y1)-(M4, Y2)
REM PLOTED DE TEMPERATURA POTENCIA SECA
M5 = XX3 + (TPEA(K) - TPEMIN) * PTPE
M6 = XX3 + (TPEA(K + 1) - TPEMIN) * PTPE
LINE (M5, Y1)-(M6, Y2)
REM PLOTED DE ENERGIA TOTAL
M7 = HHT + (HTOTAL(K) - HTMIN) * HHT
M8 = HHT + (HTOTAL(K + 1) - HTMIN) * HHT
LINE (M7, Y1)-(M8, Y2)
REM PLOTED DE AGUA PRECIPITABLE
WP1 = XX4 + W(K) * PWF + 1
WP2 = XX4 + W(K + 1) * PWF + 1
LINE (WP1, Y1)-(WP2, Y2)
NEXT K
REM PLOTED DE LINEA DE NIVELES PRINCIPALES
GOSUB 20200
RETURN

STOP
10000 REM TRABAJO
10010 REM =====
GOSUB 20000 ' APERTURA DE ARCHIVO Y LECTURA DE DATOS DE UN RADIOSONDEO
GOSUB 30000 ' CALCULOS TERMODINAMICOS NIVEL A NIVEL
GOSUB 40000 ' CALCULO DE ESPESORES (en Y mm)
GOSUB 40500 ' CALCULO DE HTOTAL (cal/gr)
GOSUB 50000 ' PERFIL DE AGUA PRECIPITABLE (mm acumulados)
IF XWORK = 0 THEN

```

```

GOSUB 6000 IMPRESION DE DATOS DE SALIDA TABLA 1
GOSUB 7000 IMPRESION DE DATOS DE SALIDA TABLA 2
GOSUB 300
END IF
IF XWORK = 0 THEN CLS
LOCATE 1, 1: PRINT RAD#
GOSUB 7500 PLOTED DE NOMBRE DE ESTACION Y FECHA
GOSUB 8000 PLOTED MARCO DE GRAFICADO
GOSUB 9000 GRAFICADO DE CURVAS
RETURN

```

```

STOP
20200 REM TRAZADO DE NIVELES PRINCIPALES
20210 REM =====
PP(0) = P(0)
FOR JZ = 0 TO NNN
REM IF PP(NNN) > P(NN) THEN GOTO 20220
FOR JK = 1 TO NN
IF P(JK) = PP(JZ) THEN JP = JK
NEXT JK
IF EGE = 2 THEN
PY1 = MARGEN + LARGOY * (P(JP) / (PMAX - PMIN))
END IF
IF EGE = 1 THEN
PY1 = MARGEN + LARGOY * (ZMAX - Z(JP)) / (ZMAX - ZMIN)
END IF
LINE (XX0, PY1)-(XX4, PY1), , , &H1
NEXT JZ
20220 REM
RETURN

```

```

21000 REM SELECTION OF RADIOSONDE DATA FILE NAME OR DEFAULT
21010 REM =====
OPEN DRIVE# + ":" + "DEFAULT.BAS" FOR INPUT AS #1
INPUT #1, DEFAULT#; CLOSE #1
FILES DRIVE# + ":*.#*"
PRINT "THE NAME OF DEFAULT DATA FILE IS "; DEFAULT#
PRINT "PRESS ESCAPE FOR DEFAULT OR PRESS ENTER FOR REAL SELECTION"
21020 X# = INKEY#; IF X# = "" THEN GOTO 21020
IF X# (<) CHR$(27) AND X# (<) CHR$(13) THEN GOTO 21020
IF X# = CHR$(27) THEN FILE# = DEFAULT#
IF X# = CHR$(13) THEN GOSUB 21030
21021 PRINT "RADIOSONDE DATA FILE NAME IS"; FILE#
RETURN

```

```

21030 REM SECTION FOR SELECTION OF RADIOSONDA NAME
21031 REM =====
CLS
SELECT# = ""
LOCATE 1, 1: PRINT "BEGIN OF SELECTION OF RADIOSONDA PLACE AND DATA"
LOCATE 3, 1: PRINT "PRESS ENTER TO SEE NEXT NAME OR ESCAPE TO SELECT"
DO UNTIL SELECT# (<) ""
IF SELECT# = "" THEN GOSUB 21500
LOOP
FILE# = SELECT#

```

RETURN

21500 REM SEARCHING FOR A FILE NAME IN THE DATA BANK

21501 REM =====

OPEN DRIVE# + ":" + "BANK.BAS" FOR INPUT AS #1

INPUT #1, NBANK

FOR I = 1 TO NBANK: PRINT

INPUT #1, TEMPO#

LOCATE 5, 1: PRINT SPACE\$(40): LOCATE 5, 1: PRINT TEMPO#

60SUB 21650

21552 A# = INKEY#: IF A# = "" THEN GOTO 21552

IF A# = CHR\$(27) THEN

SELECT# = TEMPO#

CLOSE #1

CLOSE #1

GOTO 21021

END IF

NEXT I

CLOSE #1

RETURN

21650 REM READING THE HEADER OF A RADIOSONDE DATA FILE

21651 REM =====

OPEN DRIVE# + ":" + TEMPO# FOR INPUT AS #2

INPUT #2, CM1#, CM2#

LOCATE 6, 1: PRINT SPACE\$(40): LOCATE 6, 1: PRINT CM1#

LOCATE 7, 1: PRINT SPACE\$(40): LOCATE 7, 1: PRINT CM2#

CLOSE #2

RETURN

SUB DATA#DRIVE (DRIVEDATA#)

CLS : INPUT "LETRA DEL DRIVE QUE CONTIENE LOS RADIOSONDEOS (DEFAULT ES A)"; DRIVEDATA#

IF DRIVEDATA# = "" THEN DRIVEDATA# = "A": CLS

END SUB

SUB LECTOR (NN, P1), T(), TD()

END SUB

SUB TECLA

LOCATE

END SUB

ESTACIONES RW TROPICALES

LISTADO 3

ESTACIONES TROPICALES PANAMERICANAS DE AIRE SUPERIOR
 PAN-AMERICAN TROPICAL UPPER AIR METEOROLOGICAL STATIONS

REGION IV Y III. SECTOR 23°N-25°S 110°W-29°W RW: RADIO SONDA P: PILOTO
 RG: REGION SIGL: SIGLA MT: METAR LATI: LATITUD LONG: LONGITUD SIN INFORMACION: //// //

RG	N°	NOMBRE (PAIS)	SIGL	RW	MT	LATI	LONG	HP	H/HA	TELEFON
						ggmmh	ggmmh	m	m	
IV	76458	MAZATLAN (MEXICO)	MMMZ	RW	//	2312N	10625W	////	0004	
IV	76612	GUADALAJARA (MEXICO)	MMGL	RW	//	2040N	10323W	////	1551	
IV	76644	MERIDA AEROP. INT. (MEXICO)	MMMMD	RW	//	2059N	8939W	////	0009	
IV	76654	MANZANILLO. COL (MEXICO)		RW	//	1903N	10420W	////	0003	
IV	76679	MEXICO AEROP. INT. (MEXICO)	MMM	RW	//	1926N	9905W	////	2234	
IV	76692	VERACRUZ HACIENDA (MEXICO)	MMVR	RW	//	1909N	9607W	////	0013	
IV	76723	ISLA SOCORRO. COL. (MEXICO)		RW	//	1843N	11057W	////	0035	
IV	78325	CASA BLANCA. HABANA (CUBA)	MUHA	RW	//	2310N	8221W	0050	////	
IV	78355	CAMAGUEY (CUBA)	MUCM	RW	//	2124N	7755W	0122	////	
IV	78376	GUANTANAMO ORIENTE (CUBA)	MUGM	P	//	1954N	7509W	0023	////	
IV	78384	GRAND CAYMAN AIRP. (CAYMAN ISLANDS)	MWCG	RW	//	1917N	8121W	0003	0003	
IV	78397	KINGSTON/NORMAN MANLEY (JAMAICA)	MKJP	RW	OK	1756N	7647W	0014	0003	
IV	78486	STO DOMINGO/AMERICAS (DOMINICANA)	MDS	RW	//	1826N	6953W	0014	////	
IV	78526	SAN JUAN/INT (PUERTO RICO)	TJSJ	RW	//	1826N	6600W	0019	0003	
IV	78583	BELIZE/INT AIRPORT (BELIZE)	MZBZ	RW	//	1732N	8818W	0005	0005	
IV	78641	AEROPUERTO LA AURORA (GUATEMALA)	MGGT	RW	//	1435N	9031W	1498	////	
IV	78720	TEGUCIGALPA (HONDURAS)	MHTG	RW	//	1403N	8713W	1007	////	
IV	78741	MANAGUA A.C. SANDINO (NICARAGUA)	MNMG	P	//	1209N	8610W	0056	////	
IV	78762	JUAN SANTAMARIA AEROP (COSTA RICA)	MROC	RW	//	1000N	8413W	0939	0920	
IV	78806	HOWARD AFB (PANAMA)	MPHO	RW	//	0859N	7933W	0069	0066	
IV	78861	COOLIDGE FIELD (ANTIGUA Y BARBUDA)	TAPA	RW	//	1707N	6147W	0010	////	
IV	78866	JULIANA AIRPORT (ST. MAARTEN)	TNCM	RW	//	1803N	6307W	0009	0004	
IV	78897	LE RAIZET GUADALUPE (ST MARTIN)	TFFR	RW	//	1616N	6131W	0008	0011	
IV	78925	LE LAMENTINE		P	//	1436N	6100W	0004	0004	
IV	78954	GRANTLEY ADAMS (BARBADOS)	TBPB	RW	OK	1304N	5929W	0056	0050	
IV	78970	PIARCO INT. AIRPORT. (TRINIDAD)	TTPP	RW	OK	1037N	6121W	0015	0012	
IV	78988	HATO AIRPORT (CURACAO Y TOBAGO)	TNCC	RW	OK	1212N	6858W	0067	0009	
IV	80001	ISLA SAN ANDRES (COLOMBIA)	SKSP	RW	OK	1235N	8143W	0006	0001	
III	80337	TUMACO/EL MIRA (COLOMBIA)	SKCO	RW	OK	0134N	7841W	0005	0016	
III	80222	BOGOTA/ELDORADO (COLOMBIA)	SKBO	RW	OK	0442N	7808W	2548	2547	
III	80241	GAVIOTAS (COLOMBIA)	////	RW	OK	0433N	7055W	0167	0165	
III	80398	LETICIA VASQUEZ COBO (COLOMBIA)	SKLT	RW	OK	0410S	6957W	////	0084	
III	80413	MARACAY-B. A. SUCRE (VENEZUELA)	SVBS	RW	OK	1015N	6739W	0437	0436	
III	80447	SAN ANTONIO DEL TACHIRA (VENEZUELA)	SVSA	RW	OK	0751N	7227W	0378	0377	
III	80462	SANTA ELENA DE UAIREN (VENEZUELA)	SVSE	RW	OK	0436N	6107W	0907	0907	
III	80476	LA CANADA/MARACAIBO (VENEZUELA)	SV//	RW	//	1031N	7139W	0026	0026	
III	81002	TIMEHRI (GUYANA)	SYTM	NO	OK	0630N	5815W	0030	0028	
III	81225	ZANDERIJ (SURINAME)	SMZY	P	OK	0527N	5512W	0015	////	
III	81405	CAYENNE/ROCHAMBEAU (FRENCH GUIANA)	SOCA	RW	NO	0450N	5222W	0009	0009	
III	82022	BOA VISTA AEROPORTO (BRASIL)	////	W	//	0250N	6042W	////	0140	
III	82193	BELEM (AEROPORTO)	SBBE	RW	//	0123S	4829W	0016	0016	
III	82280	SAC LUIZ (BRASIL)	SBSL	RW	//	0232S	4417W	0051	////	
III	82332	MANAUS AEROPORTO (BRASIL)	SBMH	RW	//	0309S	5959W	0084	0084	
III	82397	FORTALEZA (BRASIL)	SBFZ	RW	//	0344S	3833W	0019	////	
III	82400	FERNANDO DE NORONAH-ILHA (BRAZIL)	////	RW	//	0351S	3225W	0056	0045	

III	82599	NATAL (BRASIL)	SBNT	RW	//	0555S	3515W	0049	0049
III	82678	FLORIANO (BRASIL)	SBFO	RW	//	0646S	4301W	0123	////
III	82765	CAROLINA (BRASIL)	SBCI	RW	//	0720S	4728W	0192	////
III	82824	PORTO VELHO (BRASIL)	SBPV	W	//	0846S	6355W	////	////
III	82900	RECIFE/CURADO (BRASIL)	SBRE	RW	//	0803S	3455W	0007	0011
III	82965	ALTA FLORESTA (BRASIL)	////	RW	//	0952S	5606W	0288	////
III	82983	PETROLINA (BRASIL)	SBPL	RW	//	0923S	4029W	0370	////
III	83208	VILHENA (BRASIL)	SBVH	RW	//	1244S	6008W	////	0652
III	83229	SALVADOR (BRASIL)	SBSV	RW	//	1301S	3831W	0051	////
III	83288	BOM JESUS DA LAPA (BRASIL)	////	RW	//	1316S	4325W	0440	////
III	83378	BRASILIA AEROPORTO (BRASIL)	SBBR	RW	//	1552S	4756W	1061	////
III	83498	CARAVELAS (BRASIL)	////	RW	//	1744S	3915W	0003	////
III	83612	CAMPO GRANDE AEROPORTO (BRASIL)	SBCG	RW	//	2028S	5440W	0567	////
III	83650	TRINIDADE ILHIA (BRASIL)	////	RW	//	2030S	2919W	0005	0004
III	83746	GALEAO (BRASIL)	////	RW	//	2249S	4315W	////	0006
III	83780	SAO PAULO AEROPORTO (BRASIL)	SBSP	RW	//	2337S	4639W	0803	0802
III	83840	CURITIBA AEROPORTO (BRASIL)	SBCT	RW	//	2531S	4910W	0908	////
III	83971	PORTO ALEGRE AEROPORTO (BRASIL)	SBPA	RW	//	3000S	5111W	////	0003
III	84008	SAN CRISTOBAL-GALAPAGOS (ECUADOR)	SEGS	W	//	0054S	8936W	////	0006
III	84203	GUAYAQUIL/SIMON BOLIVAR (ECUADOR)	SEGU	W	//	0209S	7953W	0009	0004
III	84377	IQUITOS (PERU)	////	RW	//	0345S	7315W	0126	0125
III	84629	LIMA-CALLAO/AEROP. INT. (PERU)	SPIM	RW	//	1200S	7707W	0013	0013
III	85201	LA PAZ/ALTO (BOLIVIA)	SLLP	RW	//	1631S	6811W	4071	////

 RECOPIACION DE: UCV-LUIS G. HIDALGO (VER/2/29/5/93)

AN INTRODUCTION TO
DYNAMIC METEOROLOGY

Second Edition

JAMES R. HOLTON

Department of Atmospheric Sciences
University of Washington
Seattle, Washington



ACADEMIC PRESS
A Subsidiary of Harcourt Brace Jovanovich, Publishers
New York London
Paris San Diego San Francisco São Paulo Sydney Tokyo Toronto

This is Volume 23 in
INTERNATIONAL GEOPHYSICS SERIES
A series of monographs and textbooks
Edited by WILLIAM L. DONN

A complete list of the books in this series appears at the end of this volume.

which the parcel would have if expanded adiabatically to saturation. Thus, equivalent potential temperature is conserved for a parcel during both dry adiabatic and pseudoadiabatic changes of state.

In many applications tropical meteorologists prefer to use the moist static energy $h \equiv s + L_c q$, where $s \equiv c_p T + gz$ is the dry static energy. It may be shown (Problem 7) that $c_p T d \ln \theta \approx ds$ so that $c_p T d \ln \theta_c \approx dh$. Hence, moist static energy is approximately conserved when θ_c is conserved.

12.2.2 THE PSEUDOADIABATIC LAPSE RATE

The first law of thermodynamics for a moist adiabatic process (12.15) can be used to derive a formula for the rate of change of temperature with respect to height for a saturated parcel undergoing pseudoadiabatic ascent. Using the definition of θ (2.44) we can rewrite (12.15) as

$$\frac{dT}{dz} - \frac{R}{c_p} \frac{d \ln p}{dz} = - \frac{L_c}{c_p T} \frac{dq_s}{dz}$$

which with the aid of the hydrostatic equation and equation of state can be expressed as

$$\frac{dT}{dz} + \frac{g}{c_p} = - \frac{L_c}{c_p} \frac{dq_s}{dT} \frac{dT}{dz}$$

Thus, following the ascending saturated parcel we have

$$\Gamma_s \equiv - \frac{dT}{dz} = \Gamma_d [1 + (L_c/c_p) dq_s/dT] \quad (12.18)$$

where $\Gamma_d = g/c_p$ is the dry adiabatic lapse rate, and Γ_s is the pseudoadiabatic lapse rate. Since dq_s/dT is positive Γ_s is always less than Γ_d . In the mid-troposphere Γ_s is about 6°C km^{-1} .

12.2.3 CONDITIONAL INSTABILITY

We showed in Section 2.7.3 that for dry adiabatic motions the atmosphere is statically stable; provided that the lapse rate is less than the dry adiabatic lapse rate (i.e., the potential temperature increases with height). If the lapse rate Γ lies between the dry adiabatic and pseudoadiabatic values ($\Gamma_s < \Gamma < \Gamma_d$) the atmosphere is stably stratified with respect to dry adiabatic displacements but unstable with respect to pseudoadiabatic displacements. Such a situation is referred to as *conditional instability* (i.e., the instability is conditional to *saturation* of the air parcel).

The conditional stability criterion can also be expressed in terms of the gradient of θ_c^* , where θ_c^* is defined as the equivalent potential temperature

12.2 CUMULUS CONVECTION

of a hypothetically saturated atmosphere which has the thermal structure of the actual atmosphere. Thus,

$$d \ln \theta_c^* = d \ln \theta + d(L_c q_s/c_p T) \quad (12.19)$$

where T is the actual temperature, *not* the temperature after adiabatic expansion to saturation as in (12.17). To derive this condition we consider the motion of a saturated parcel in an environment in which the potential temperature is θ_0 at the level z_0 . At the level $z_0 + \delta z'$ the undisturbed environmental air thus has potential temperature

$$\theta_0 - \frac{\partial \theta}{\partial z} \delta z'$$

Suppose a saturated parcel which has the environmental potential temperature at $z_0 + \delta z'$ is raised to the level z_0 . When it arrives at z_0 the parcel will have potential temperature

$$\theta_1 = \left(\theta_0 - \frac{\partial \theta}{\partial z} \delta z' \right) + \delta \theta$$

where $\delta \theta$ is the change in potential temperature due to ascent through vertical distance $\delta z'$. Assuming a pseudoadiabatic ascent we see from (12.16) that

$$\frac{\delta \theta}{\theta} \approx - \delta \left(\frac{L_c q_s}{c_p T} \right) \approx - \frac{\partial}{\partial z} \left(\frac{L_c q_s}{c_p T} \right) \delta z'$$

so that the buoyancy of the parcel when it arrives at z_0 is proportional to

$$\frac{\theta_1 - \theta_0}{\theta_0} \approx - \left[\frac{1}{\theta} \frac{\partial \theta}{\partial z} + \frac{\partial}{\partial z} \left(\frac{L_c q_s}{c_p T} \right) \right] \delta z' \quad (12.20)$$

Now the first term on the right in (12.20) refers to conditions in the environment, while the second refers to the saturated parcel. However, provided that the parcel temperature is not too different from that of the environment, the two terms on the right may be combined with the aid of (12.19) to provide an expression for the buoyancy in terms of θ_c^* :

$$\frac{\theta_1 - \theta_0}{\theta_0} \approx - \frac{\partial \ln \theta_c^*}{\partial z} \delta z'$$

Now, the saturated parcel will be positively buoyant at z_0 provided $\theta_1 > \theta_0$. Thus the conditional stability criterion for a *saturated* parcel is

$$\left. \begin{array}{l} \frac{\partial \theta_c^*}{\partial z} < 0 \text{ conditionally unstable} \\ \quad \quad = 0 \text{ saturated neutral} \\ \quad \quad > 0 \text{ absolutely stable} \end{array} \right\} \quad (12.21)$$

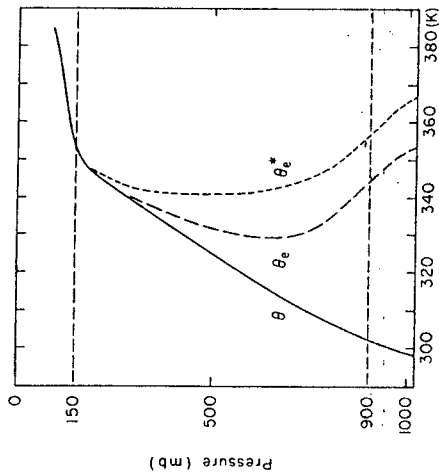


Fig. 12.1 Typical sounding in the tropical atmosphere showing the vertical profiles of potential temperature θ , equivalent potential temperature θ_e , and the equivalent potential temperature θ_e^* of a hypothetically saturated atmosphere with the same temperature at each level. (After Ooyama, 1969. Reproduced with permission of the American Meteorological Society.)

In Fig. 12.1 the vertical profiles of θ , θ_e , and θ_e^* for a typical tropical sounding are shown. It is obvious from the figure that the mean tropical atmosphere is conditionally unstable in the lower and middle troposphere. However, this observed profile does not imply that convective overturning will spontaneously occur in the tropics. The release of conditional instability requires not only $\partial\theta_e^*/\partial z < 0$, but also a saturated atmosphere, and the mean relative humidity in the tropics is well below 100%. Thus, low-level convergence with its resultant forced ascent or vigorous vertical turbulent mixing in the boundary layer is required to produce saturation. The amount of ascent necessary to produce a positively buoyant parcel can be estimated simply from Fig. 12.1. A parcel rising pseudoadiabatically from a level $z_0 - \delta z'$ will conserve the value of θ_e characteristic of the environment at $z_0 - \delta z'$. Now, the buoyancy of a parcel depends only on the difference in density between the parcel and the environment. Thus, in order to compute the buoyancy of the parcel at z_0 , it is not correct simply to compare θ_e of the environment at z_0 to $\theta_e(z_0 - \delta z')$ because if the environment is unsaturated the difference in θ_e for the parcel and the environment may be due primarily to the difference in mixing ratios, not to any temperature (density) difference. To estimate the buoyancy of the parcel $\theta_e(z_0 - \delta z')$ should instead be compared to $\theta_e^*(z_0)$, which is the equivalent potential temperature which the environment at z_0 would have if it were isothermally brought to saturation. The

parcel will thus become buoyant when $\theta_e(z_0 - \delta z') > \theta_e^*(z_0)$, for then the parcel temperature will exceed the temperature of the environment. From Fig. 12.1 we see that θ_e for a parcel raised from 1000 mb will intersect the θ_e^* curve just above 900 mb, whereas a parcel raised from any level much above 900 mb will not intersect θ_e^* no matter how far it is forced to ascend. It is for this reason that *low-level convergence* is required to initiate convective overturning in the tropical atmosphere. Only air near the surface has a sufficiently high value of θ_e to become buoyant when it is forcibly raised. Of course, convergence at higher levels may play an important role in maintaining the convection by adding substantial moisture to the system.

12.2.4 THE SLICE METHOD

In the parcel method the environment is assumed to remain undisturbed by the convective parcels. In reality the rising motion in the convection must be compensated by subsidence in the environment if an overall mass balance is to be maintained. For this reason, the parcel method tends to overestimate the degree of instability of the atmosphere. More significantly, it is the compensating subsidence and adiabatic warming in the environment which is the direct cause of the large-scale heating associated with cumulus convection in synoptic scale disturbances. The simplest manner in which to take account of this adjustment in the environment is the so-called *slice method*. In this method it is assumed that on any horizontal plane the upward mass flux in the convection cells is just balanced by downward mass flux in the environment immediately surrounding the convection cells. This mass balance may be expressed as follows: We let ρ' and w' be the density and vertical velocity in the convection cells and ρ and w be the corresponding fields in the environment. If the fractional horizontal area occupied by the convection cells is designated by a , then for mass balance

$$\rho'w'a = \rho w(1 - a) \quad (12.22)$$

Now suppose that in a time increment δt the convective parcels rise an amount $\delta z'$ and the environment sinks by δz . We can write

$$w' \approx \frac{\delta z'}{\delta t}, \quad w \approx \frac{\delta z}{\delta t}$$

Substituting into (12.22) and neglecting the small difference between ρ' and ρ we obtain

$$a \delta z' \approx (1 - a) \delta z \quad (12.23)$$

We now consider the difference at a level z_0 between the temperatures of a saturated parcel which has risen from the level $z_0 - \delta z'$ and the environmental air which has sunk from the level $z_0 + \delta z$. Letting θ_0 be the initial



**GUEST LECTURES on
Convection**

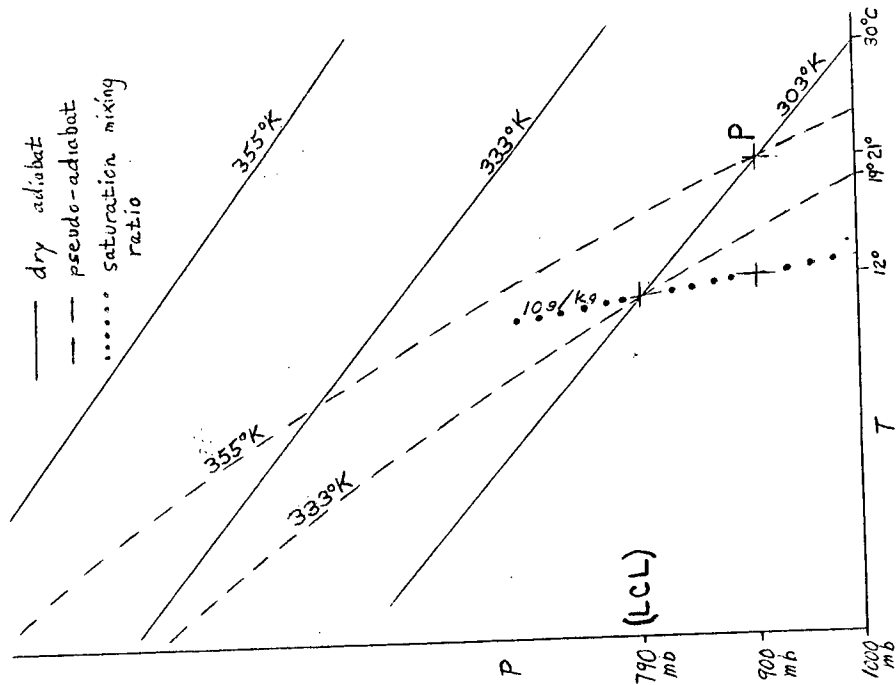


Fig. 1. Thermodynamic diagram showing the relationship between thermodynamic quantities for $P = 900\text{mb}$, $T = 21^\circ\text{C}$, $T_d = 10^\circ\text{C}$. It follows that $\theta = 303^\circ\text{K}$, $\theta_E = 333^\circ\text{K}$, $\theta_w = 292^\circ\text{K}$, and $\theta_E^* = 355^\circ\text{K}$.

The definitions are easily demonstrated on the schematic thermodynamic diagram shown in Fig. 1. As an example, we consider an air parcel P defined by: $P = 900\text{mb}$, $T = 21^\circ\text{C}$, $T_d = 10^\circ\text{C}$. Then, the dry adiabat through P gives $\theta = 303^\circ\text{K}$. The moist adiabat through P gives $\theta_E^* = 355^\circ\text{K}$. The moist adiabat through the LCL for parcel P gives $\theta_E = 333^\circ\text{K}$; tracing this adiabat down to the surface yields the approximate wet-bulb potential temperature as $\theta_w = 292^\circ\text{K}$ (19°C).

For most practical purposes, we may state that a parcel conserves:

- a. θ during unsaturated parcel processes
- b. θ_E during both unsaturated and saturated parcel processes
- c. θ_E^* during saturated parcel processes.

Thus a description of a tropical sounding in terms of θ , θ_E and θ_E^* is useful. A typical example is shown in Fig. 2.

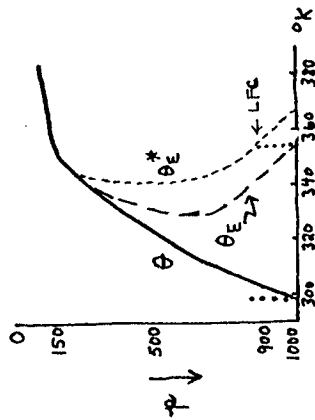


Fig. 2. Typical vertical profiles of θ , θ_E and θ_E^* in the tropical atmosphere. These curves imply conditional instability up to about 500 mb and convective instability up to 700 mb.

casting and cumulus parameterization problems, especially on shorter time scales. (Recall that, in Fig. 2 the layer of conditional instability is considerably deeper than that of convective instability).

Fig. 2 may also be used to trace an upward moving air parcel. The parcel initially follows the two dotted vertical lines in Fig. 2, corresponding to the conservation of θ and θ_E by the initially unsaturated parcel. After the LCL is reached, θ for the parcel begins to increase until the LFC is reached, at which point the θ of the parcel and environment are equal. Since the parcel is saturated, it follows that the LFC occurs where

$$(\theta_E)_{\text{parcel}} = (\theta_E)_{\text{environment}}$$

Thus the crossing of the dotted vertical line (conservation of θ_E by the parcel) with the θ_E^* sounding curve determines the location of the LFC. This criterion may also be stated in terms of the moist static energy profiles, of course. (Arakawa, et.al., 1968, Madden and Robitaille, 1970).

Finally, Fig. 3 shows smoothed vertical profiles of θ_E for disturbed and undisturbed regimes for a land and ocean station in the tropics. We see that θ_E possesses a pronounced minimum (and hence convective instability) in mid-troposphere during undisturbed periods for both the land and ocean examples. Regions of disturbed weather are marked by a considerably lessened lapse of θ_E . Over the land station this is due mainly to a decrease of surface values during disturbed (cloudy) periods. In contrast, the main change takes place as an increase in mid-tropospheric values over the ocean location.

We note the following:

a) θ never decreases with height

$$\frac{\partial \theta}{\partial z} \geq 0 \quad \text{or} \quad \Gamma \leq \Gamma_m$$

so the sounding is stable for dry processes. (Here Γ and Γ_m

are the moist static energy and moist static energy of the environment, respectively)

height

$$\frac{\partial \theta_E^*}{\partial z} < 0 \quad \text{or} \quad \Gamma > \Gamma_m$$

so the sounding implies conditional instability in that layer.

Since θ_E^* depends upon the temperature distribution alone,

this condition is equivalent to a lapse rate in excess of the moist adiabatic lapse rate;

b) between the surface and about 700 mb θ_E decreases with height

$$\frac{\partial \theta_E}{\partial z} < 0$$

so the sounding implies convective instability in that layer.

Since θ_E depends upon the vertical distribution of both

temperature and water vapor, this condition cannot be expressed in terms of temperature lapse rates alone.

It is true that the vertical profile of θ_E tends to resemble those

of θ_E^* . In some papers, the θ_E profile is used to define regions

of conditional instability; from the above definitions this is, strictly speaking, incorrect. However, the pseudo-adiabatic lifting of a layer to saturation will result in a conditionally unstable layer ($\frac{\partial \theta_E^*}{\partial z} < 0$)

if $\frac{\partial \theta_E}{\partial z} < 0$, and so the distinction between the two variables is

sometimes ignored. On the other hand, the differences in the profiles

of θ_E and θ_E^* are probably of great importance for the tropical fore-

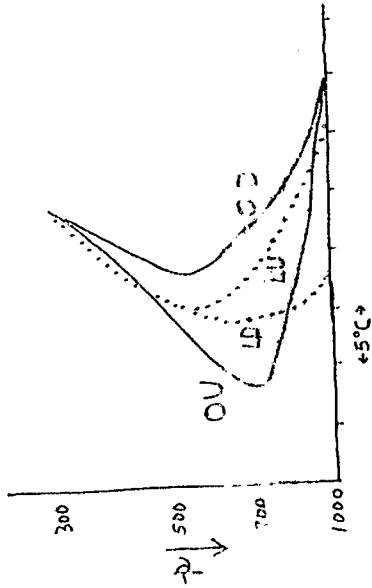


Fig. 3. Vertical profiles of θ_E for disturbed (D) and undisturbed (U) periods for a land (L) and ocean (O) station in the tropics. Abscissa is in relative units since curves have been shifted so as to coincide at 300mb.

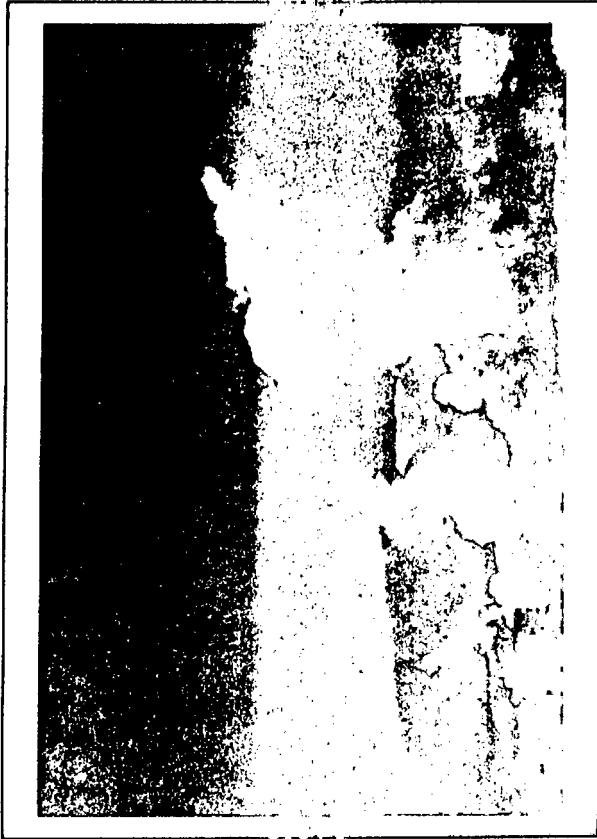
References

Arakawa, A., K. Katayama, and Y. Mintz, 1968: Numerical simulation of the general circulation of the atmosphere. In Proc. WMO-IUGG Symposium on Numerical Weather Prediction, Tokyo, Japan.

Garstang, M., N.E. LaSeur, and R. Hadlock, 1970: Results from a comprehensive tropical field experiment. Extended abstract in Proc. Symposium on Tropical Meteorology, Abstracts, Univ. of Hawaii, Honolulu, Hawaii, June, 1970.

Huschke, R.E., ed., 1959: Glossary of Meteorology, American Meteorological Society, Boston, Mass.

Madden, R.A., and F.E. Robitaille, 1970: A comparison of the equivalent potential temperature and the static energy. J. Atm. Sci., 27, 327-329.



NOTES from
the Workshop
on Cumulus Parameterization

"We may achieve climate, but weather is thrust upon us." - O. Henry

Climatology of the Trade-Wind Inversion in the Caribbean

MURRAY GUTNICK

Geophysics Research Directorate, Air Force Cambridge Research Center¹

(Original manuscript received 13 August 1957; revised manuscript received 24 February 1958)

ABSTRACT

Three years of twice-daily raobs for the midseason months at six stations on the Caribbean were analyzed for evidence of the trade-wind inversion. The seasonal, spatial, or diurnal variation of the various parameters which constitute the inversion regime (frequency, height of the base, strength, thickness, and moisture budget) is discussed. It was found that most of the parameters showed a distinct seasonal variation but little or no spatial or diurnal variations.

1. Introduction

Since its discovery in 1856 by Piazzzi-Smyth [6], the trade-wind inversion has been investigated by many meteorologists, notably Sverdrup [8] and Von Ficker [10]. Von Ficker published a climatological analysis of the trade-wind inversion of the Atlantic Ocean utilizing the 217 kite soundings of the Meteor expedition (1925-27) and some older observations. Although the Meteor soundings were made mainly during the Northern Hemisphere summer and were essentially limited to the area east of 50 deg W long in the Atlantic, Von Ficker extended his analysis to the extreme eastern Caribbean by utilizing a few soundings taken at Barbados and the Lesser Antilles during the early 1900's [1]. Local characteristics of the inversion in the Caribbean have been reported in various studies by Stone [9] and others [2], but no comprehensive survey of the phenomenon has been published. Recent questions about the significance of the inversion in electromagnetic propagation, cloud seeding, aerial photography, *etc.*, have encouraged the author to undertake the climatological analysis of the Caribbean trade-wind inversion. Specifically, the seasonal, spatial, and diurnal variations (if any) of the following parameters of the trade-wind inversion were desired:

1. Frequency.
2. Topography (height).
3. Thickness (vertical extent).
4. Strength (temperature difference between the base and top of the inversion).
5. Moisture distribution through the inversion.
6. Moisture content of the air above and below the inversion.

¹ Most of this paper was prepared while the author was affiliated with Headquarters, Air Weather Service, Washington, D. C.

2. Data

Radiosonde data for six stations in the Caribbean were utilized in this investigation. The stations selected were:

1. Guantanamo Bay NAS, Cuba (19 deg 54 min N, 75 deg 01 min W). This station is located in the heart of the trade-wind region of the Caribbean area.
2. Swan Island (17 deg 24 min N, 83 deg 56 min W), at the western periphery of the Caribbean.
3. Coolidge AFB, Antigua (17 deg 07 min N, 61 deg 47 min W), at the eastern periphery.
4. Grand Bahama Island (26 deg 37 min N, 78 deg 22 min W), at the northern edge of the area.
5. Trinidad NAS (10 deg 41 min N, 61 deg 37 min W), at the southern edge of the region.
6. Albrook AFB, Balboa, Canal Zone (8 deg 56 min N, 79 deg 34 min W), at the extreme southwestern portion of the Caribbean.

Actually, Albrook AFB is not representative of the trade-wind regime during the warmer months of the year, since at this time the Canal Zone is located within the classical climatological concept of the doldrum belt. Raobs taken at 0300 and 1500 GCT for January, April, July, and October for each of the stations were analyzed (additional months were analyzed in cases where some salient feature of the trade-wind inversion was not apparent in the four selected midseason months). In all cases a 3-year record for each of the midseason months was used: for Antigua the period of record was 1946, 1947, and 1949; for Trinidad 1953-1955; and for all other stations 1951-1953. There were relatively few days when the raob data were missing. Of the 4478 possible

ascents, only about 15 per cent was missing. The missing data were randomly distributed.

3. Method

The method used in the investigation was straightforward. After selecting the stations and period of record, both surface and upper-air maps for the selected periods of record were examined in order to ascertain if there were any abnormal features in the general circulation patterns during those months; no such anomalies were apparent. Next, each raob was carefully analyzed for evidence of the trade-wind inversion (at levels below 500 mb). Only those raobs which showed the trade-wind inversion were selected for analysis (all other types of inversions such as radiational, frontal, *etc.*, were excluded). Whenever a raob showed the subsidence inversion typical of the trades (an abrupt decrease of relative humidity and mixing ratio in the inversion layer), the relative humidity and mixing ratio at both the 1000- and 500-mb levels were noted. Also noted were the temperature, relative humidity, mixing ratio, and height at the base and top of the inversion. Then the following parameters were summarized by month and hour:

1. Mean relative humidity and mixing ratio between the 1000-mb level and the base of the inversion. This was considered to be the mean of the layer between the 1000-mb surface and that of the base of the inversion ($\overline{RH}_{1000}^b, \overline{w}_{1000}^b$).
2. Mean relative humidity and mixing ratio between the top of the inversion and the 500-mb level. Similarly this was considered to be the mean of the layer between the top of the inversion and that of the 500-mb level ($\overline{RH}_T^{500}, \overline{w}_T^{500}$).
3. Mean height of the base of the inversion (Z_b).
4. Mean thickness of the inversion (difference in height between the base and the top of the inversion, ΔZ).
5. Relative humidity and mixing-ratio difference between the base and top of the inversion (Δr and ΔRH).
6. Strength of the inversion (difference in temperature between the base and top of the inversion, ΔT).

If an isothermal layer showed the characteristic drop in humidity between the base and top, it was included as an inversion. Calculations of the humidity variation between the base and the top of the inversion and of the humidity be-

tween the top and the 500-mb level posed something of a problem. That is, in many cases the relative humidity values from the top of the inversion to the 500-mb level were reported as "motor boating." This "motor boating" was assumed to be caused by the inability of the humidity element in the radiosonde to function at very low relative humidities. For example, at -10°C the humidity element will "motor boat" if the relative humidity is less than 25 per cent. Thus, in order to obtain some index of the moisture content at the top of the inversion and at higher levels, the relative humidity which will cause "motor boating" for a given temperature was recorded. In other words, if the temperature at the top of the inversion was -10°C and the relative humidity was reported as "motor boating," a relative humidity of 25 per cent was recorded for this point. This, of course, gives an overestimation of the humidity since, conceivably, the humidity can be lower than that associated with the cut-off temperature. Thus, in this study the values of the difference in relative humidity and mixing ratio between the base and the top of the inversion are probably too small. Also, the mean mixing ratio and relative humidity values between the top of the inversion and the 500-mb level are probably too high.

In all other respects the radiosonde data were recorded as indicated; no correction was incorporated for instrumental errors, lag, *etc.*

4. Frequency of inversions

The mean percentage frequency of inversions (0300 to 1500 GCT) and the percentage frequency for the individual years that comprise the mean are given in fig. 1. Despite the variations in the magnitude of inversion frequency from station to station, the seasonal trends throughout the area are essentially similar; that is, the trade-wind inversion occurs most frequently during winter and least frequently during summer or autumn. The transition from one season to another, however, is not gradual and smooth. At some time during the spring, depending upon the station, the inversion frequency decreases abruptly from its cold-season maximum to its warm-season minimum. The autumn, to winter transition is

TABLE 1. Mean frequency of the trade-wind inversion at Guantanamo Bay (0300 and 1500 GCT).

	Jan	Apr	May	July	Oct	Nov
Frequency (per cent)	85	65	45	44	34	59

also abrupt. For example, table I illustrates the abrupt change in frequency from April to May and from October to November.

The abrupt changes in inversion frequency during the transitional season as indicated by the data may be partially attributed to the method of defining the trade-wind inversion. That is, in the study only those cases where a layer exhibited either no change of temperature with height or an increase of temperature with height, associated with a sharp decrease of moisture content within

the layer, were counted as a trade-wind inversion. During the transitional season, particularly in spring, there were many cases of layers within which the temperature decreased slightly and the moisture decreased markedly with height; these cases were not tabulated as trade-wind inversions. If, however, these cases had been tabulated as trade-wind inversions, the change in inversion frequency during the transitional months would not be as abrupt as indicated by the data, particularly during the spring.

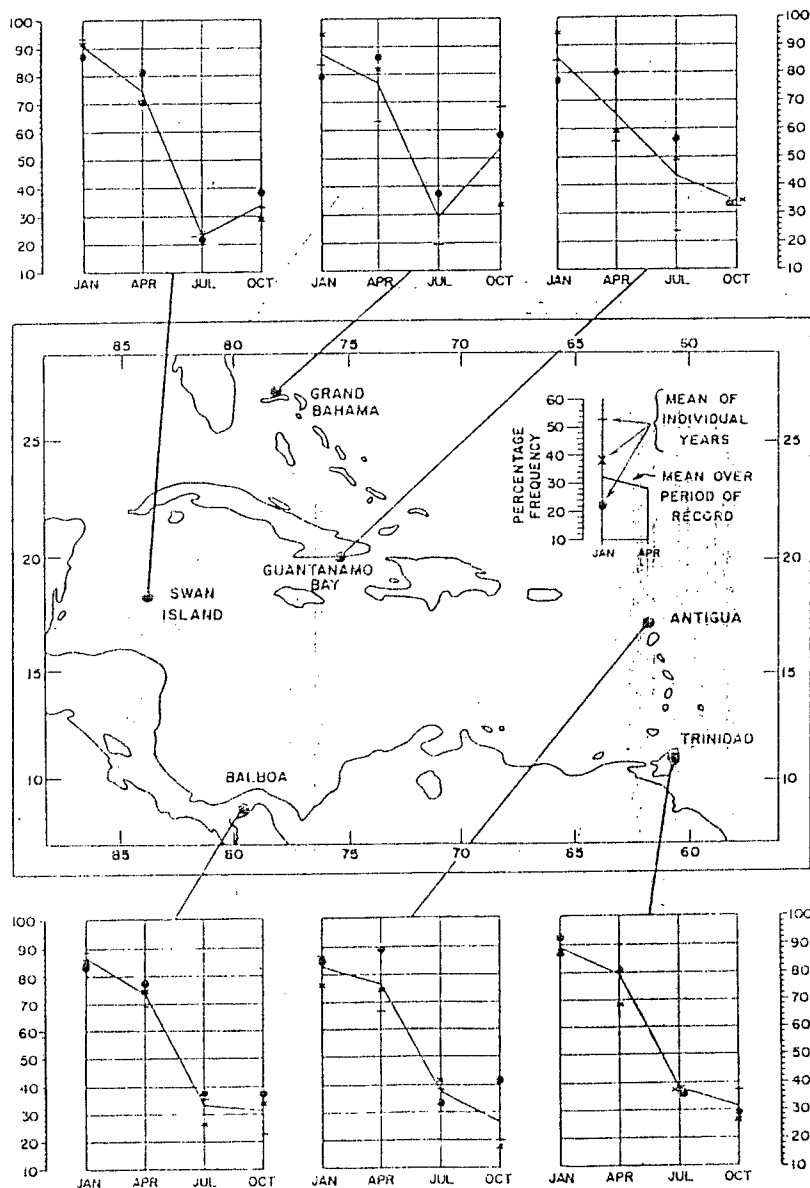


FIG. 1. Percentage frequency of the trade-wind inversion.

At any particular locality, year-to-year variations from the mean in the frequency of the trade-wind inversion are relatively small, particularly in winter; on the average, the greatest variability occurs in spring and autumn. For example, the average variation in frequency from the mean value for all stations combined is 4 per cent in January, 9 per cent in April, 5 per cent in July, and 7 per cent in October. The extreme maximum variation from the mean for any one year (21 per cent) occurred in Guantanamo Bay in July.

Insofar as the diurnal variation in frequency is concerned, it is negligible during all months of the year (when the frequency of inversions at 0300 and 1500 GCT was compared, it was found that there was not a consistent observable difference).

During winter the inversion frequency increases slightly from east to west; there is no consistent north-south variation. However, in all other seasons there is no systematic meridional or zonal variation. Surprisingly enough, the trade-wind inversion during summer is just as prevalent in the area classically delineated as the doldrums (Balboa) as in the heart of the Caribbean trades. This, however, is probably an anomalous condition peculiar to Balboa and not representative of the doldrum belt in general. That is, there is cold water south of Panama so that with a southerly flow a stratum of cold air may be advected into the area producing an inversion which is not truly a trade-wind inversion. Also, there exists at this station a peculiar diurnal variation in the winds aloft at lower levels which appears to be connected with topographic influences.

It might be well to mention at this time a characteristic of summer inversions in the area. During the colder months the trade inversion can be thought of as a continuous sheet. However, during the summer the inversion is discontinuous. That is, it appears here and there locally, and appears to be predominantly associated with the subsiding side of migratory disturbance.

5. Strength of the inversion

When contrasted with the inversion of the North Atlantic east of about 45 deg W, the trade-wind inversion of the Caribbean is weak indeed. Von Ficker's maps representing mainly Northern Hemisphere summer conditions indicate the difference in temperature between the base and top of the inversion ranges from an average of 5C near the Cape Verde Islands to about 2C near the eastern Caribbean. In contrast, the strength of the inversion during July (see table 2 for the seasonal variations of ΔT) at all the Caribbean stations is less than 1.1C. Actually, the Meteor data and the data of table 2 are not strictly comparable, since the Meteor data were taken over the undisturbed trade-wind flow of the open ocean while the raob data presented here probably reflect some "heated-island" influence [5]. However, the order of magnitude differences between Von Ficker's maps and table 2 cannot be accounted for by the "heated-island" effect, especially if the contrast is made between the undisturbed trade-wind flow and small flat islands such as Swan Island or Antigua. The maximum ΔT in the North Atlantic as indicated by Von Ficker was 22C, while the maximum observed ΔT in the Caribbean was found to be 10C (Guantanamo Bay, in April).

The seasonal trend of ΔT is similar to that of the inversion frequency. That is, the strongest inversions occur during winter and the weakest inversions occur during summer or autumn. In January the mean value of ΔT in the Caribbean varies from 1.4 to 2.5C, while during July the range is 0.5 to 1.0C. Year-to-year variations in the mean value of ΔT are small in all seasons. The average variation of ΔT from the mean value for all stations combined is 0.4C in January, 0.3C in April, 0.2C in July and in October. The extreme maximum variation from the mean for any one year was 1.0C (Grand Bahama, in January). Day-to-day variations in ΔT are also small. Table

TABLE 2. Difference in temperature (in degrees centigrade) between the base and the top of the inversion (0300 and 1500 GCT).

	January				April				July				October			
	A	B	C	M	A	B	C	M	A	B	C	M	A	B	C	M
Guantanamo Bay	1.3	1.9	2.3	1.8	0.6	0.6	1.8	1.0	0.6	0.6	0.8	0.7	0.1	0.6	0.7	0.5
Grand Bahama	1.6	2.1	3.5	2.5	1.3	2.2	2.5	2.0	0.5	0.5	0.8	0.6	0.8	1.3	1.6	1.2
Swan Island	1.7	1.5	1.8	1.7	1.4	1.4	1.8	1.5	0.5	0.5	0.8	0.6	0.5	0.6	1.0	0.7
Balboa	1.2	2.1	0.8	1.4	1.0	0.7	1.2	1.0	0.2	0.6	0.7	0.5	0.3	0.3	0.8	0.5
Antigua	1.2	1.4	1.6	1.4	1.5	1.5	1.8	1.6	1.4	1.0	0.6	1.0	0.1	0.5	0.1	0.2
Trinidad	1.4	1.3	2.3	1.6	0.9	0.8	1.4	1.0	0.5	0.6	0.9	0.7	0.4	0.3	0.7	0.5

A, B, and C refer to the mean of individual years while M is the mean for the 3-yr period.

3 gives a frequency distribution of the daily values of ΔT for three representative stations. As can be seen from table 3, approximately 73 per cent of all ΔT 's during January at Grand Bahama are between 0 and 4C (the mean monthly value is 2.5C); in July all values of ΔT are between 0 and 4C. All other stations show a similar small scatter about the mean monthly values of ΔT .

TABLE 3. Percentage frequency distribution of the strength of the inversion (0300 and 1500 GCT).

	Temperature difference ΔT in degrees centigrade							
	0	1	2	3	4	5	6	7
January								
Grand Bahama	7	21	25	13	7	10	5	11
Guantanamo Bay	29	19	21	13	9	4	5	0
Balboa	40	25	15	11	4	2	2	1
April								
Grand Bahama	17	22	36	13	6	1	2	0
Guantanamo Bay	41	30	18	6	3	1	0	2
Balboa	37	40	14	8	1	1	0	0
July								
Grand Bahama	46	43	9	0	2	0	0	0
Guantanamo Bay	60	24	13	1	1	0	0	0
Balboa	61	31	9	0	0	0	0	0
October								
Grand Bahama	40	37	12	2	4	5	0	0
Guantanamo Bay	75	15	7	3	0	0	0	0
Balboa	56	40	4	0	0	0	0	0

Comparison of the 0300 GCT with the 1500 GCT raobs for indication of the diurnal variation of ΔT shows no consistent systematic diurnal variation for any season. This is illustrated in table 4 for three representative stations.

The spatial variation of ΔT is very small. In all seasons, ΔT decreases slightly from north to south. There is no systematic east-west variation except during summer when ΔT is slightly larger in the eastern Caribbean. It should be borne in

mind that the spatial and diurnal variations of ΔT are so small between stations or between observational hours that they can conceivably be attributed to reasons such as instrumental errors, rounding-off effects, etc.

6. Height of the base of the inversion

The seasonal trends of all stations show one common characteristic: the inversion is highest during summer (see table 5). At all stations except Balboa, Z_b is slightly lower in spring than in winter. Whether this decrease in Z_b from winter to spring is real or whether it is merely due to the relatively short period of record used is not known.

TABLE 4. Diurnal variations of the average strength (degrees centigrade) of the inversion.

Station	Time (GCT)	Jan	Apr	July	Oct
Antigua	0300	1.3	1.7	1.1	0.0
	1500	1.5	1.4	0.8	0.4
Swan Island	0300	1.6	1.4	0.5	0.6
	1500	1.7	1.6	0.6	0.8
Grand Bahama	0300	2.5	1.8	0.6	1.2
	1500	2.5	2.1	0.6	1.2

Year-to-year variations in the mean height of the base of the inversion are relatively large but not extreme. The average variation in height of the mean of individual years from the mean over the period of record for all stations combined is 770 ft in January, 630 ft in April, 1000 ft in July, and 570 ft in October. Day-to-day variations in Z_b are very large. Table 6 gives a frequency distribution of the daily values of Z_b for three stations:

Of all the stations, Swan Island during October has the smallest variability of Z_b . At this station, approximately 17 per cent of the daily values of Z_b are within 1000 ft of the mean monthly value (7525 ft). The maximum variability of Z_b occurs at Antigua in July. Here, only about 4 per

TABLE 5. Mean height (in feet) of the base of the inversion (0300 and 1500 GCT).

	January				April				July				October			
	A	B	C	M	A	B	C	M	A	B	C	M	A	B	C	M
Guantanamo Bay	6600	6800	9100	7500	6300	7200	7500	7000	6700	8600	9100	8125	8200	7300	8500	8000
Grand Bahama	7400	5600	6300	6425	6900	6100	5300	6100	8300	9500	10,500	9425	7800	8900	8100	8275
Swan Island	7000	7600	8400	7675	7000	8400	5000	6800	7400	8800	9200	8475	7100	7500	8000	7525
Balboa	6600	7500	8200	7425	7200	8800	7000	7675	6900	8600	9000	8175	6800	8400	7500	7575
Antigua	7600	9400	8900	8625	6700	8400	7400	7500	7600	10,800	7600	8675	6100	7900	8400	7475
Trinidad	8500	8300	11,000	9275	7600	8300	7400	7775	14,400	10,200	12,500	11,875	9000	10,100	10,800	10,075

A, B, and C refer to the mean of individual years while M refers to the mean for the 3-yr period of record.

cent of the daily values are within 1000 ft of the mean monthly value (8675 ft). Comparison of the 0300 GCT with the 1500 GCT raobs reveals that there is no consistent, systematic diurnal variation of Z_b at any time of the year.

The spatial variation of Z_b is rather peculiar. There is no significant zonal variation at any time. However, during January and April the inversion is somewhat higher in the south as contrasted to the north. If Grand Bahama, Swan Island, and Balboa are compared for Z_b during July, we find that Z_b decreases from north to south. In contrast, if Antigua and Trinidad are compared during the same month, we find that Z_b at Trinidad is approximately 3700 ft higher. This peculiar spatial variation is also apparent during October.

7. Thickness of the inversion

The vertical extent of the inversion is the only parameter of the inversion regime that shows no

consistent systematic seasonal variation (see table 7 for the seasonal distribution of ΔZ). For example, at both Antigua and Trinidad ΔZ is at a minimum during autumn, but it is at a maximum at Antigua during summer and at Trinidad during winter. At Swan Island, Guantanamo Bay, and Grand Bahama, ΔZ is at a minimum during summer; however, the maximum occurs at Guantanamo in winter and at the other two stations during spring. At Balboa the inversion is thickest in winter and thinnest in spring.

The mean value of ΔZ does not change much from one year to another. For example, the average deviation of the mean value of ΔZ from the mean over the period of record for all stations combined is less than 75 ft in all seasons except summer when the value is 110 ft. The day-to-day variations of ΔZ are considerable. Table 8 is a frequency distribution of the thickness of the inversion for three stations where the variability of

TABLE 6. Percentage frequency distribution of the average height (feet) of the inversion (0300 and 1500 GCT).

	≤1000	1001-2000	2001-4000	4001-6000	6001-8000	8001-10,000	10,001-13,000	13,001-16,000	>16,000 feet
January (per cent)									
Swan Island	0	1	6	21	35	21	9	4	2
Antigua	0	0	2	15	33	25	15	9	1
Trinidad	0	0	4	16	32	19	16	7	7
April									
Swan Island	0	9	14	23	21	18	8	5	2
Antigua	0	0	3	13	37	35	12	0	0
Trinidad	0	0	8	29	24	13	15	9	2
July									
Swan Island	0	5	19	10	25	5	18	10	8
Antigua	0	0	3	45	7	3	10	20	13
Trinidad	0	0	0	2	21	7	14	30	25
October									
Swan Island	2	3	21	16	18	12	16	5	7
Antigua	0	0	11	43	18	8	11	11	0
Trinidad	0	0	10	19	17	6	10	15	23

TABLE 7. Mean thickness (in feet) of the inversion (0300 and 1500 GCT)

	January				April				July				October			
	A	B	C	M	A	B	C	M	A	B	C	M	A	B	M	
Guantanamo Bay	1300	1240	1400	1320	1040	920	970	975	1240	850	600	900	840	1300	1220	1120
Grand Bahama	740	920	790	820	890	920	700	840	760	770	700	725	710	900	830	810
Swan Island	730	980	880	860	960	820	960	910	590	760	760	700	830	820	690	780
Balboa	880	1060	760	890	570	820	800	730	700	920	910	840	940	730	590	750
Antigua	950	970	1050	990	870	1030	1030	980	970	1280	970	1070	990	906	880	920
Trinidad	920	720	990	890	800	860	810	850	770	900	810	830	690	770	830	760

A, B, C refer to the mean of individual years while M refers to the mean for the 3-yr period of record.

ΔZ is relatively large, moderate, and small (Guantanamo Bay, Grand Bahama, and Trinidad, respectively).

TABLE 8. Percentage frequency distribution of the thickness (in feet) of the inversion (0300 and 1500 GCT).

	≤200	201-400	401-800	801-1200	1201-1600	>1600 feet
January (per cent)						
Guantanamo Bay	2	6	29	22	15	26
Grand Bahama	7	16	35	24	10	8
Trinidad	1	16	35	31	10	8
April						
Guantanamo Bay	4	13	37	23	12	12
Grand Bahama	1	18	35	24	18	4
Trinidad	0	10	40	33	12	6
July						
Guantanamo Bay	1	17	43	23	9	7
Grand Bahama	1	17	47	21	6	6
Trinidad	2	7	46	30	7	7
October						
Guantanamo Bay	0	3	22	44	17	14
Grand Bahama	0	11	45	31	2	11
Trinidad	2	8	50	35	6	0

Consider Guantanamo during July. Here, about 36 per cent of all values of ΔZ are within 200 ft of the mean value (900 ft). At Trinidad during April, 39 per cent of all values of ΔZ are within 200 ft of the monthly mean (850 ft).

There is no apparent diurnal variation in the thickness of the inversion layers. Spatially, Z does not vary zonally in any season nor meridionally in any season but summer. During summer the inversion thickness decreases somewhat from east to west.

8. Moisture budget of the inversion

The moisture budget of the trade-wind inversion is probably the most interesting parameter of the inversion regime. The moisture distribution can be subdivided into three categories—the variations in moisture below the inversion, through the inversion, and above the inversion. Let us first consider the variations below the inversion (see fig. 2 and table 9). As can be seen from these data, both the relative humidity and mixing ratio from 1000 mb to the base of the inversion exhibit little change throughout the year. For example, at the station that exhibits the greatest seasonal change in relative humidity (Balboa) the relative humidity ranges from 74 per cent in winter to 83 per cent in summer; also, the mixing ratio at the station with the greatest seasonal change (Grand Bahama) ranges from 8.9 g per kg in January to 12.3 g per kg during July (an in-

crease of 40 per cent). At all other stations, however, the percentage increase in mixing ratio from its minimum monthly value to its maximum value averages 22 per cent. The variation of mixing ratio and relative humidity from year to year and even from day to day is small. Spatial and diurnal variation in both the mixing ratio and relative humidity below the base of the inversion is negligible.

Next, observe the seasonal change in relative humidity and mixing ratio from the base to the top of the inversion (see fig. 3 and table 10). The change in both these parameters decreases from colder to warmer weather. There is no significant diurnal or spatial variation.

Finally, consider the seasonal moisture distribution from the top of the inversion to the 500-mb level (see fig. 4 and table 11). It is obvious that there is a marked seasonal change; both the relative humidity and mixing ratio are at a minimum during cold weather and at a maximum during warm weather. Although the actual magnitude of the increase in mixing ratio from colder to warmer weather is essentially similar from the 1000-mb level to the base of the inversion and from the top of the inversion to the 500-mb level (they both increase about 2 g per kg), the increase in moisture above the inversion cannot be accounted for by the increase in moisture below. That is, if in order to obtain an order of magnitude it is assumed that the mixing ratio below the inversion is increased by 2 g per kg from winter to summer, then by using the "parcel" method we find that the increase in mixing ratio from winter to summer above the inversion is less than 1 g per kg (much less than is indicated by the data). The question then arises as to the mechanism by which the upper layers gain relatively large amounts of moisture from colder to warmer weather while the lower layers exhibit little or no change. The most obvious process is, of course, vertical transport from below (convection).

It has been hypothesized [7] that, as convection increases, active clouds penetrate the base of the inversion and evaporate in the dry air above. In this way, moisture is introduced into the lower portions of the inversion layer. As convection continues, the clouds push farther into the inversion and bit by bit the whole inversion is raised. As a corollary to this hypothesis, the following features should theoretically be observed as convection increases (winter to summer):

1. The height of the base of the inversion should rise.
2. The strength should decrease.

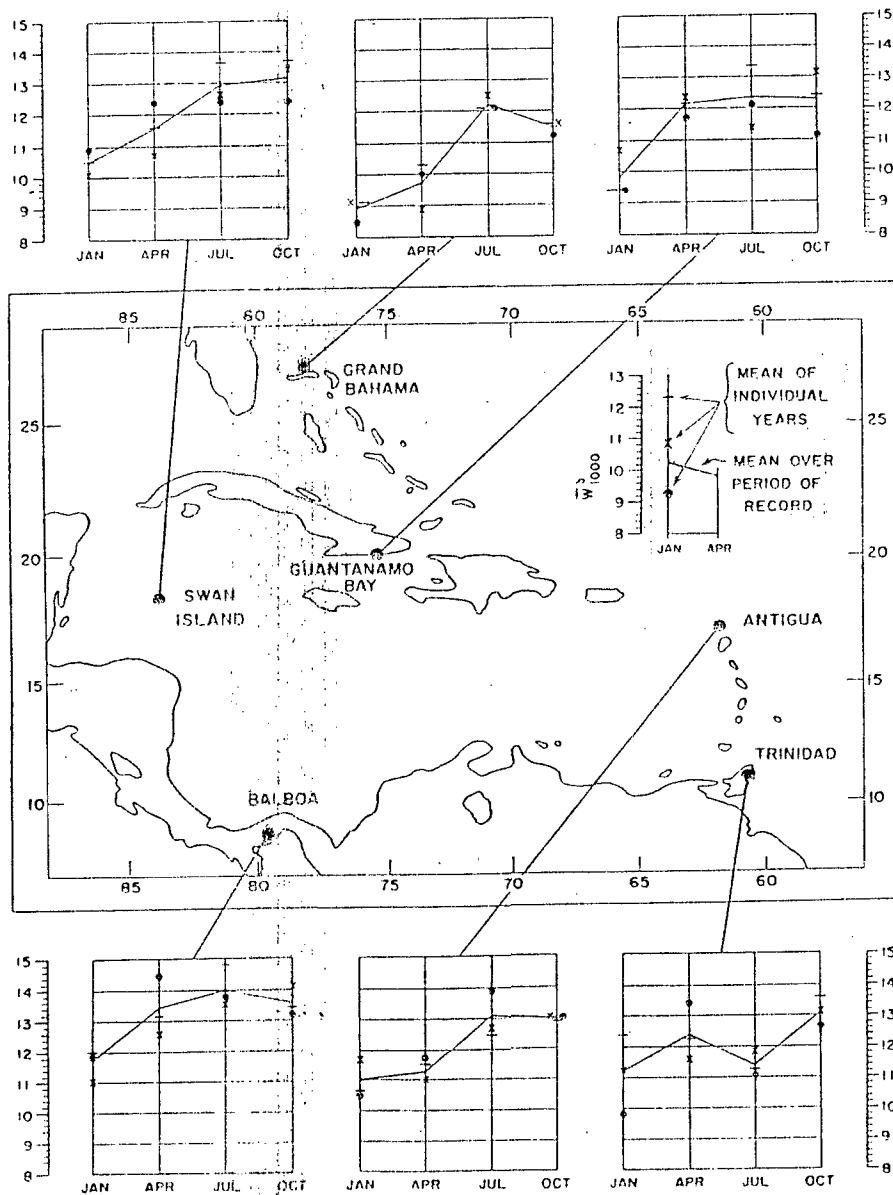


FIG. 2. Mean mixing ratio g per kg between 1000 mb and the base of the inversion.

TABLE 9. Mean relative humidity (in per cent) between 1000 mb and the base of the inversion (0300 and 1500 GCT).

	January				April				July				October			
	A	B	C	M	A	B	C	M	A	B	C	M	A	B	C	M
Guantanamo Bay	73	65	72	70	72	76	74	74	76	67	70	71	75	70	71	72
Grand Bahama	71	78	78	76	76	72	74	74	75	75	76	75	74	77	83	77
Swan Island	67	73	73	71	67	70	71	69	72	75	75	74	77	83	72	77
Balboa	76	74	72	74	76	73	80	76	83	81	84	83	79	86	79	81
Antigua	75	77	70	74	75	73	74	74	77	81	82	80	78	77	79	78
Trinidad	77	74	70	70	78	76	75	74	74	78	72	75	79	79	82	80

A, B, and C refer to the mean of individual years while M refers to the mean for the 3-yr period of record.

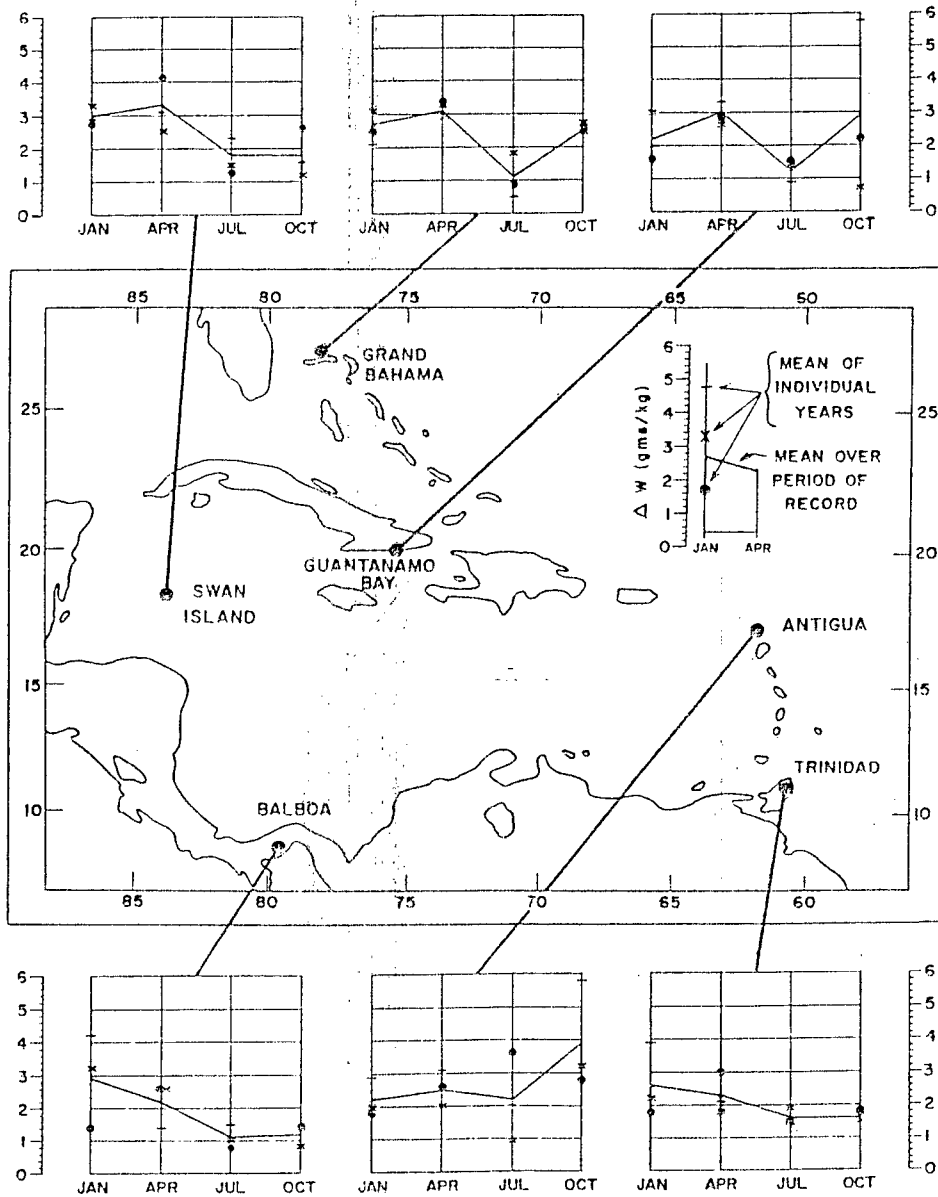


FIG. 3. Difference in mixing ratio g per kg between the base and top of the inversion.

TABLE 10. Difference in relative humidity (per cent) between the base and top of the inversion (0300 and 1500 GCT).

	January				April				July				October			
	A	B	C	M	A	B	C	M	A	B	C	M	A	B	C	M
Guantanamo Bay	35	36	34	35	27	24	32	28	15	19	19	18	20	20	24	21
Grand Bahama	33	45	39	39	49	19	24	21	12	25	20	19	27	37	33	32
Swan Island	33	38	39	37	15	18	18	17	18	20	24	21	16	10	27	18
Balboa	41	36	17	31	17	28	27	24	16	14	16	15	13	10	18	14
Antigua	37	24	28	30	29	29	30	30	33	19	31	28	33	28	45	35
Trinidad	32	33	24	30	28	33	28	20	28	24	24	24	22	19	19	20

A, B, and C refer to the mean of individual years while M refers to the mean in the 1-yr period of record.

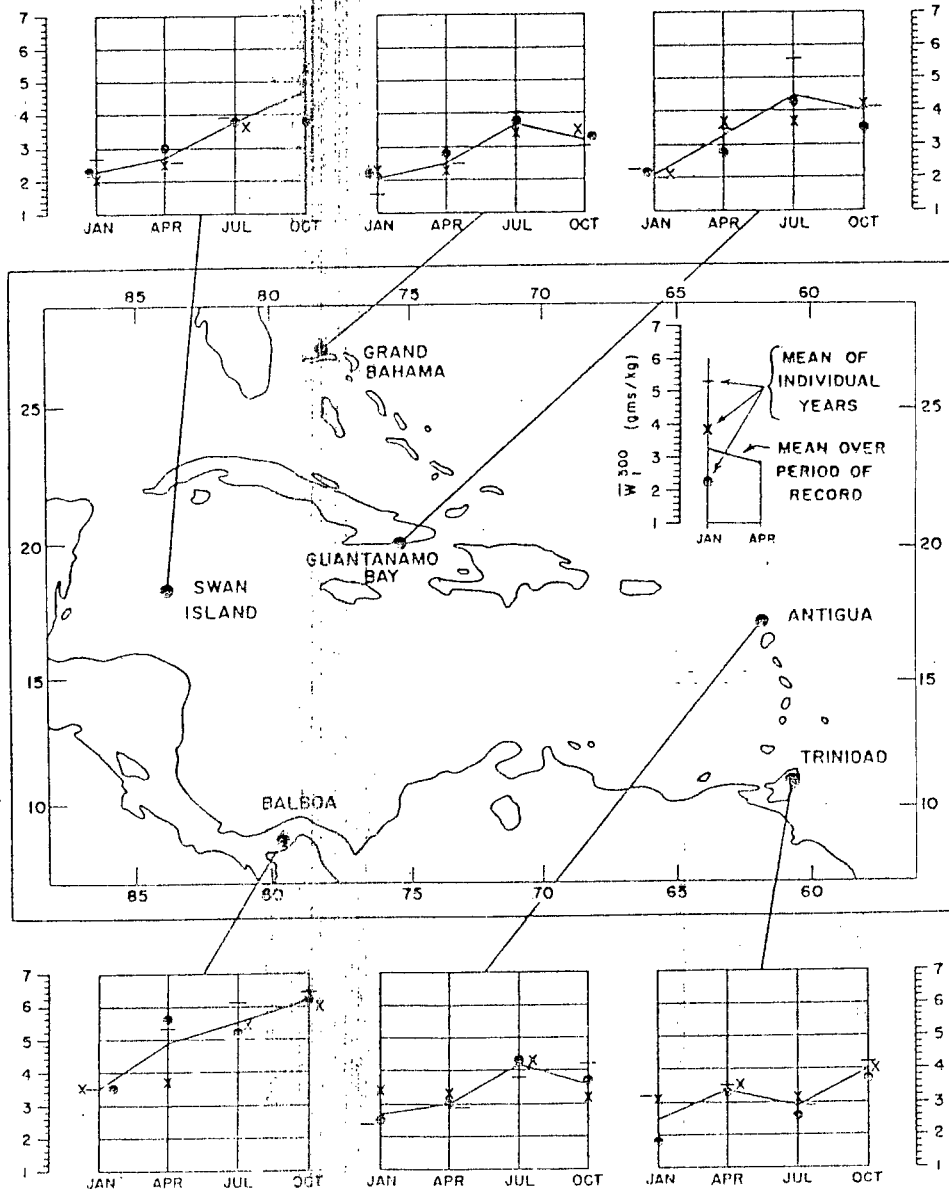


FIG. 4. Mean mixing ratio h^2 per kg between the top of the inversion and the 500-mb level.

TABLE II. Mean relative humidity (in per cent) between the top of the inversion and the 500-mb level (0300 and 1500 GCT).

	January				April				July				October			
	A	B	C	M	A	B	C	M	A	B	C	M	A	B	C	M
Guantanamo Bay	29	25	29	28	35	40	32	36	54	43	47	48	42	43	34	40
Grand Bahama	26	29	34	29	32	33	32	34	50	42	52	48	38	46	43	42
Swan Island	31	24	29	28	28	24	28	28	44	46	45	45	49	60	40	50
Balboa	39	34	43	39	47	39	45	44	67	63	59	63	70	69	68	69
Antigua	29	39	31	31	31	37	31	33	56	64	53	56	55	36	41	44
Trinidad	36	36	26	31	47	39	40	48	47	41	45	50	50	57	52	

A, B, and C refer to the mean of individual years while M refers to the mean in the 3-yr period of record.

3. The difference in relative humidity and mixing ratio from the base of the inversion to the top should decrease.
4. The relative humidity and mixing ratio above the inversion should increase.

From the previously presented data it is apparent that all these features do occur; therefore, it appears that the convection theory fits the observable statistics. However, superficially there appears to be an argument against the convection theory as follows.

The Caribbean is approximately 1400 n mi wide. Assuming that air travels from the eastern Caribbean to the western Caribbean at 15 km, it would take approximately 4 days to complete its journey. If the assumption is made that air is constantly subjected to strong convection in its 4-day journey, it would follow that the features observed seasonally should occur spatially; that is, the height of the base of the inversion should increase and the strength decrease, etc., downstream. Since most of the data do not indicate such a spatial variation, it apparently follows that the convective theory does not altogether fit the observable facts. However, Jacobs [3, 4] has demonstrated that the net increase of sensible heat and moisture in air moving across the Caribbean is negligible. Thus, no significant spatial variation should be expected.

Although the convection theory fits all the observable data in itself, it is almost certain that the increase in convection from winter to summer is coupled with a decrease from winter to summer in divergence and subsidence in the layer of air above the inversion.

Another explanation of seasonal increase in moisture in the upper layer could conceivably be horizontal advection of moisture into the layer. This hypothesis does not appear likely since, with the high value of wind constancy over the area, it would be expected that a strong meridional moisture gradient would exist. The generally

weak gradient over the Caribbean as indicated by table II and fig. 4 does not support this position. Therefore, the only reasonable explanation of the mechanism of the seasonal moisture distribution of the inversion regime is the convection theory coupled with decreased subsidence from winter to summer.

Acknowledgments.—The writer wishes to express thanks to the members of the Directorates of Scientific Services and Climatology, Headquarters Air Weather Service, for their constructive criticisms and suggestions. Extremely valuable comments were given by Mr. R. G. Stone and Capt. Earl C. Kirdle, Headquarters Air Weather Service; Dr. Herbert Riehl, University of Chicago; Mr. Lester Hubert, U. S. Weather Bureau; and Dr. Raymond Wexler, Woods Hole Oceanographic Institution.

REFERENCES

1. Air Corps Tactical School, 1942: *Caribbean Weather Characteristics*. Montgomery, Alabama, U. S. Military-Naval Services, 5-106.
2. Dunn, G. E., 1940: Cyclogenesis in the tropical Atlantic. *Bull. Amer. meteor. Soc.*, 21, 215-229.
3. Jacobs, W. C., 1943: Sources of atmospheric heat and moisture over the North Pacific Ocean. *Annals N. Y. Acad. of Sci.*, 44, 19-40.
4. —, 1950: The distribution and some effects of the seasonal quantities of E-P (evaporation minus precipitation) over the North Atlantic and North Pacific. *Archiv meteor. Geophys. Bioklim.*, Ser. A, 2, 1-16.
5. Malkus, J. S., 1955: The effects of a large island upon the trade-wind stream. *Quart. J. r. meteor. Soc.*, 81, 538-550.
6. Pizzari-Smyth, C., 1858: Astronomical experiment on the peak of Teneriffe. *R. Soc. London, Philosoph. Trans.*, 48, 465-533.
7. Riehl, H., 1954: *Tropical meteorology*. New York, McGraw-Hill Book Co., Inc., 275-278.
8. Sverdrup, H. V., 1917: Der nordatlantische passat. *Veröf. des Geophys. Inst. der Univ. Leipzig, Zweite Serie*, 2, 1-96.
9. Stone, R. G., 1942: *Scientific survey of Puerto Rico and the Virgin Islands, Vol. 19*. New York, N. Y. Acad. Sci., 126 pp.
10. Von Ficker, H., 1936: Die passat-inversion. *Veröf. des Meteor. Inst. der Univ. Berlin*, 1, No. 4.

ABOUT OUR MEMBERS

AMS members participating in the Atmospheric Electricity Conference in Portsmouth, N. H., in May were: C. E. Anderson, D. Atlas, H. J. aufm Kamp, M. Brook, H. R. Byers, Seville Chapman, R. M. Cunningham, D. R. Fitzgerald, J. W. Ford, Milton Greenberg, H. Hatakeyama, R. E. Holzer, H. Israel, T. Kitada, J. MacCreedy, Jr., C. B. Moore, F. A. Rich, F. J. Suter, S. P. Venkateshwaran, R. Vonnegut, and H. J. Gunn.

U. S. Weather Bureau Superior Accomplishment Awards were made in May to Lorenz C. Armstrong for excellent work in the Central Office Management Section and to Dale R. Harris of the Central Office Observations and Station Facilities Division for his accomplishments as project leader on the Newark ANDB Project.

Morton L. Barad, A. Nelson Dingle, and Wendell E. Hewson were contributing authors in the JOURNAL OF THE AIR POLLUTION CONTROL ASSOCIATION for May 1958. Dr. Barad's article was entitled *An Analysis of Diffusion Methods*. Professors Dingle and Hewson collaborated on *An Experimental Study of Ragweed Pollen Penetration*.